Texas Tech University

Master's Report

The Permian Basin:

A Brief Overview

PETR 6001

April, 2014

Prepared By:

Kyle Blackwell

Abstract:

The purpose of this report is to familiarize the reader with the Permian Basin. In this report, a brief geological history of the tectonics that formed the Permian basin, from Pre Cambrian through Permian time, are introduced. In addition, the resulting present day geology of the now subsurface formations is described. Information concerning hydrocarbon bearing formations, including stratigraphic columns, cross sections, and production history is provided to allow the reader to familiarize themselves with the Permian Basin. The information is broken down into conventionally producing formations and unconventionally producing formations, as well as by geographic location. Finally, a case study of an emerging area of interest in an unconventional enhanced recovery formation is presented. The case study introduces the reader to the oil bearing Wolfcamp shale in the Midland Basin. Included is an assessment of porous and permeable rock, hydrocarbons in place, as well as an evaluation of geomechanical properties to determine if the formation is susceptible to stimulation.

Table of Contents

Table of Tables

Table of Figures

Introduction to the Permian Basin:

The Permian Basin is an area of oil-and-gas production located in West Texas and adjoining southeastern New Mexico. The Permian Basin received its name because it contains some of the world's thickest deposits of rock from the Permian geologic period. It covers an area approximately 250 miles wide and 300 miles long, and contains producing formations such as the Yates, San Andres, Clear Fork, Spraberry, Wolfcamp, Yeso, Bone Spring, Avalon, Canyon, Morrow, Devonian and Ellenberger. Not all producing formations located in the Permian basin were formed during the Permian Period however. Many formations, such as the Strawn, Woodford, Barnett and Ellenberger have much older origins. Oil and natural gas production range in depth from a few hundred feet up to five miles below the surface. The Permian Basin is a significant oil-producing area, producing approximately 295 million barrels of oil in 2011, and 312 million barrels in 2012. To date, the Permian Basin has produced over 29 billion barrels of oil and 75 trillion cubic feet of gas, and industry experts estimate recoverable oil and natural gas resources exceeding what has been produced since its discovery in 1921. Increased use of enhanced-recovery practices has produced substantial increases in oil production.

In Texas, the Permian basin is comprised of more than 7,000 Railroad Commission (RRC) fields, and production is divided into districts, 7C, 08 and 8A, as seen in the figures below. The 59 Texas counties as well as 5 New Mexico counties that make up the Permian Basin are listed in tabular format below as well. The majority of current development can be attributed to certain fields, however.

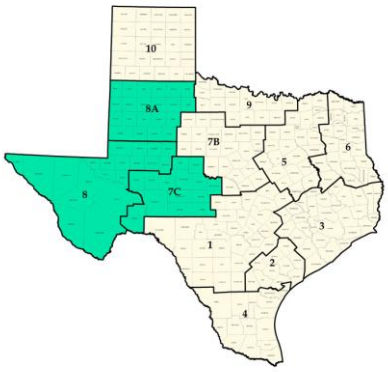

Figure 1 - Permian Basin Texas Districts (RRC)

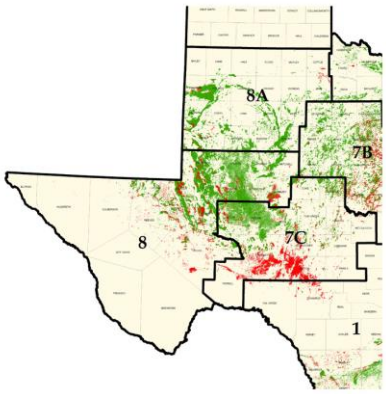

Figure 2 - Permian Basin Oil and Gas Production (RRC)

Total cumulative oil production (1921 to present):
28,478,229,290 (approximately 29 billion barrels)

According to the Texas Railroad Commission, for the calendar year 2012, which is the most recent total production year available, the Permian Basin crude oil production accounted for 57 percent of Texas' total statewide crude oil production, approximately 430 million barrels. Also, the Permian Basin accounted for 51 percent of the Texas statewide liquid production, which includes condensate, at 509 million barrels. The Permian Basin accounts for roughly 14 percent of the total U.S. annual production, or 2 billion barrels according to the U.S. Energy Information Administration (EIA). Overall, the state of Texas represents about 25 percent of U.S. total annual crude oil production (TX RRC).

Table 1 - List of Texas Permian Basin Counties

PERMIAN BASIN COUNTIES, TX		
ANDREWS	HOCKLEY	NOLAN
BORDEN	HOWARD	PECOS
COCHRAN	IRION	REAGAN
COKE	JEFF DAVIS	REEVES
CRANE	KENT	SCURRY
CROSBY	KIMBLE	STERLING
DAWSON	LAMB	TERRY
DICKENS	LOVING	TOM GREEN
ECTOR	LUBBOCK	UPTON
GAINES	LYNN	WARD
GARZA	MARTIN	WINKLER
GLASSCOCK	MIDLAND	YOAKUM
HALE	MITCHELL	

Table 2 - List of New Mexico Permian Basin Counties

PERMIAN BASIN COUNTIES, NM		
CHAVES	LEA	ROOSEVELT
EDDY	OTERO	

Origins of the Permian Basin:

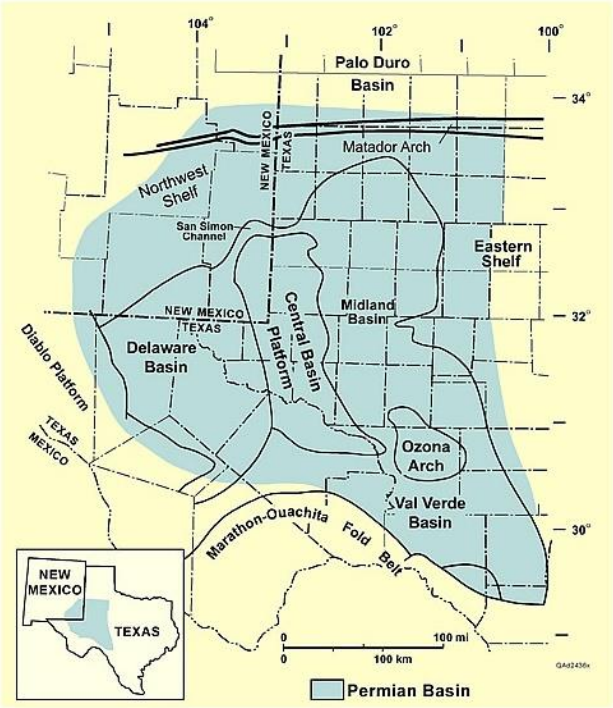

Figure 3 - Highlighted Permian Basin Region (USDOE)

The Permian Basin is divided into three main structural areas. First, the Central Basin Platform (CBP), is a NW-trending uplifted basement block that separates the Delaware Basin (to the west) from the Midland Basin (to the east). This uplift occurred during the Pennsylvanian period. Prior to the uplift, the two basins and the CBP were relatively low relief features, within a shallow Paleozoic-age basin, known as the Tobosa Basin. Following the uplift of the CBP, and the development of the two individual basins, the Tobosa Basin ceased to exist. As a result of the uplifted basement blocks, deeper reservoir horizons, such as the Ellenburger Formation, are much shallower, which greatly improves the economics of wells and fields along this structure.

During Wolfcampian time, the CBP uplift ceased, and a regional erosional unconformity developed that beveled off the tops of underlying structures. Above the unconformity, carbonate reefs were deposited on the relatively flat erosional surface. As a result, underlying fold and thrust structures became capped by flat-lying carbonate reservoirs. This created stratigraphic trap reservoirs along with deeper structural traps, creating a complex system of numerous pay zones that greatly increase the economic potential of drilling in this area.

The northern termination of the CBP is the San Simon Channel, and the Northwest Shelf. The Northwest Shelf is a broad depositional shelf that extends northward from the Midland Basin to the Matador Arch. The San Simon Syncline is a narrow sag that separates the CBP from the Northwest Shelf. The southern termination of the CBP is the Val Verde Basin, which was a result of the tectonics of the

Marathon Fold-and Thrust Belt during the Pennsylvanian and Early Permian periods. The Val Verde Basin is filled with more than 15,000 feet of flysch and clastic rocks derived from the Marathon thrust sheets.

Second, The Midland Basin is located to the east of the CBP. The cross section of the Midland Basin, taken perpendicular to the basin axis, is slightly asymmetric and deepens to the west. The western boundary contains complex faults and folds that formed along the eastern margin of the CBP. The eastern boundary, designated the Eastern Shelf, is relatively indistinct. The Eastern Shelf represents a gradual rise from the deeper western part of the basin. Therefore, the eastern boundary of the Midland basin is fairly arbitrary.

Finally, The Delaware Basin contrasts strongly and is significantly deeper than the Midland Basin. The Delaware Basin is more asymmetric, and deepens to the east. The greater burial depth and organic rich sediment influx means that there is greater thermal maturity and much deeper hydrocarbon reserves. As a result, much of the hydrocarbon reserves have developed into natural gas. The western margin of the Delaware Basin is bounded by a Tertiary-age Salt Flat Graben. Further to the west lies the Diablo Platform, which developed alongside the Central Basin Platform (Hoak).

A Brief Tectonic History of the Permian Basin (SEPM STRATA/USGS):

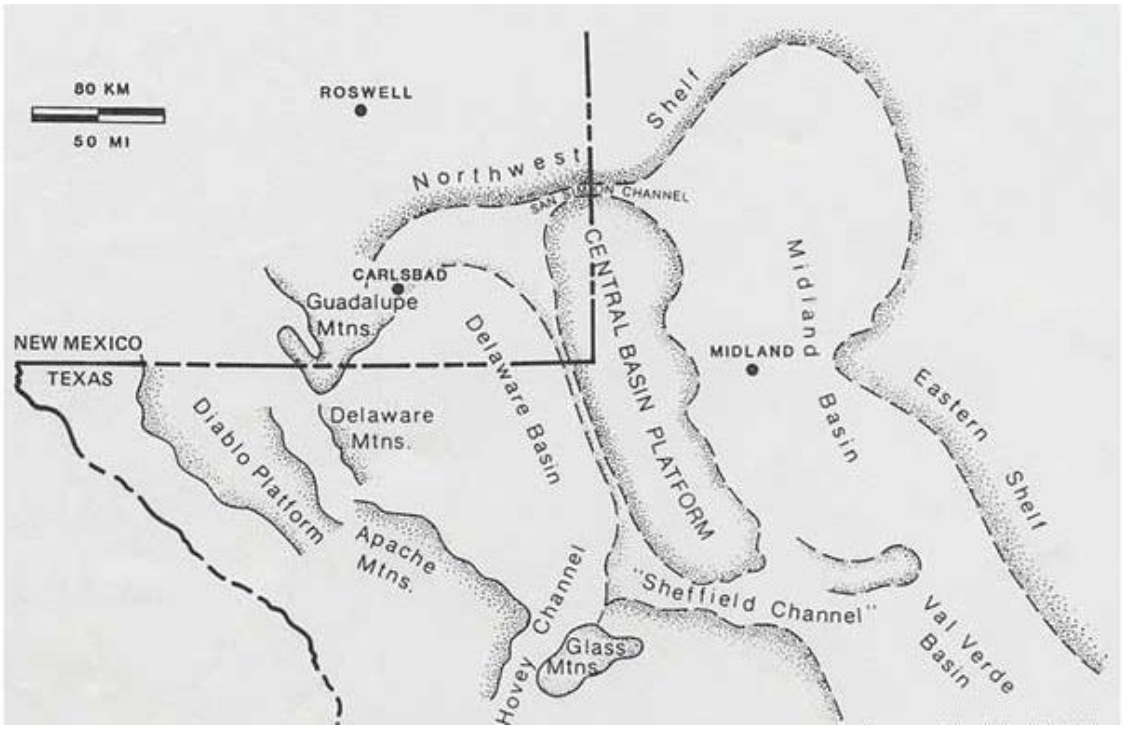

Figure 4 - Permian Basin during the Late Permian (SEPM STRATA)

The structural development of the Permian Basin has direct implications on the accumulation and preservation of vast hydrocarbon reserves. Understanding the tectonic development of the Permian Basin will provide insight into the development of both source rock and reservoir formations. The development of the Permian Basin is generally divided into three stages: the first encompassing the

Cambrian through Mississippian Periods, in which the region was a broad marine basin, known as the Tobosa basin, in which vast accumulations of carbonate and clastics were deposited. The second stage of the Permian Basin tectonic development was initiated by the Hercynian Orogeny, in which the North American Craton collided with the South American/ African continent, Gondwana, during the Early Pennsylvanian through Early Permian periods. This second stage caused the Tobosa Basin to differentiate into deep basins surrounded by shallow shelves. The third stage was initiated when the basin became structurally stable, and vast deposits of clastics were deposited in the deep basins, while carbonates were also being deposited on the shallow shelves.

Tectonic Timeline:

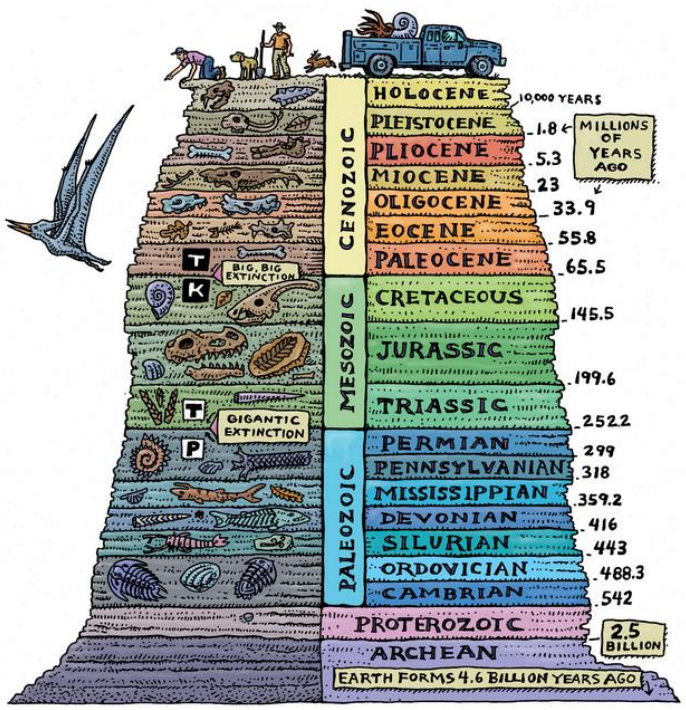

Figure 5 - Geologic Time Scale (Troll)

Stage One: 'Passive Margin,' Late Precambrian to Mississippian (850-331 ma.)

-During stage one, development of the Tobosa Basin, a broad, gently dipping depression occurred, in which sedimentation consisted of uniform shelf carbonates and thin basinal shales.

Figure 6 - Tobosa Basin: by the end of Mississippian, the Delaware, Central, and Midland basins developed (SEPM STRATA)

Precambrian and Cambrian –

The Tobosa Basin, formed due to subsidence, created a flat coastal plain across which the Early Ordovician, or Ellenburger, Sea progressed to the Northwest.

Lower Ordovician –

The Ellenburger Sea spread a wedge of evenly bedded shelf carbonates across the Tobosa Basin as it spread to the Northwest. The carbonate shelves were wide and shallow, and cross-shelf circulation was limited. As a result, most of the carbonate was dolomitized soon after deposition. Also, as a result of sea progression, the sediments thin from nearly 2,000 feet thick at the southern end of the basin to zero feet north of the present day Delaware Basin.

Middle Ordovician –

During this time period, the sandstone, carbonate and shale sediments which make up the Simpson formation were deposited. This formation is comprised of about fifty percent shale, and reaches thicknesses of up to 2,000 feet.

Late Ordovician, Silurian, and Devonian –

As subsidence continued, the Northwest trending axis of the Tobosa Basin was too deep for extensive carbonate deposition. As a result, chert and shale deposition occurred. The shale deposited during this time period contained large amounts of organic material, which has been preserved as carbonaceous residue.

Early Mississippian –

Slight uplift and erosion which occurred during the Late Devonian Period exposed the Upper Ordovician, Silurian and Devonian deposits. As the sea transgressed, the Woodford shale, an important source rock for pre-Mississippian reservoirs, was deposited.

Middle-to-Late Mississippian –

During this period, deposits covering most of the Southern Tobosa Basin consist mostly of shale. Deposits along the axis of the Tobosa sag reach thicknesses of up to 7,000 feet. The shale deposits filled the uplifted Devonian depressions and surrounding shelf areas. Also, the Tobosa Basin developed a median ridge, which split the basin into the Delaware and Midland basins, laying way for the present Permian Basin structure.

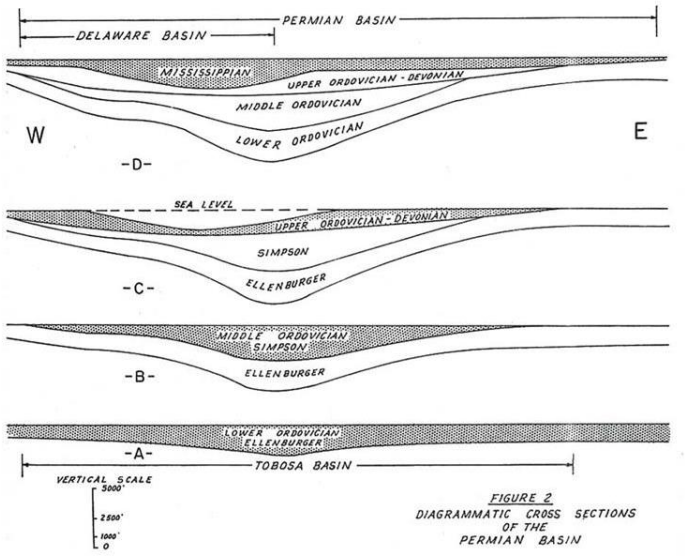

Figure 7 - Permian Basin Cross Section, from Early Ordovician to Mississippian (SEPM STRATA)

Stage Two: 'Collision Phase,' Late Mississippian to Pennsylvanian (331-299 ma.)

-During stage two, the Hercynian orogeny, which was the result of the collision of the North American craton and the South American/ African continent, Gondwana, gave rise to the Ouachita-Marathon fold belt. This fold belt deformed the Tobosa Basin greatly along basement faults and existing weak zones. Rapid subsidence, faulting and sedimentary filling of the two existing depressions gave rise to the Northwest trending Delaware and Midland foreland basins, as well as the Central Basin and Diablo

platforms. Broad carbonate shelves formed along the western, northern and eastern margins of the Permian Basin Sea, while eroded clastics from the platforms were deposited in the basins.

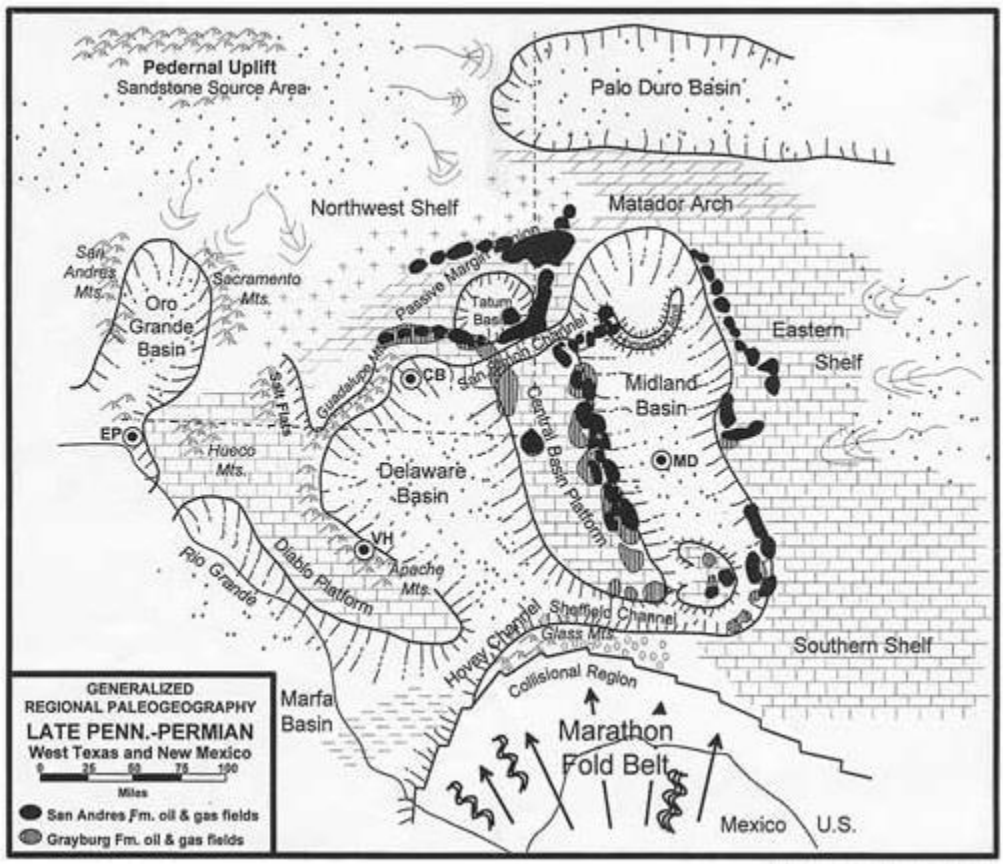

Figure 8 - Major Basin and Shelf Elements, Late Pennsylvanian to Permian (SEPM STRATA)

Late Mississippian –

During this period, the eastern edge of the Delaware basin subsided along the Central Basin uplift, causing the Delaware Basin to dip to the east. Northeast-southwest tectonic compressional forces caused faulting and folds to form which caused the Central Basin uplift to rise, forming the Central Basin Platform and separating the Delaware and Midland basins.

Early Pennsylvanian –

This was a period of rapid basin subsidence. The Delaware Basin deepened greatly, which prevented deposition of carbonates. Clastic deposition was limited to the northern and northwest margins of the Permian Basin. The central and southern basin areas were largely without sediment deposition, except for some shale.

Middle and Late Pennsylvanian –

This was a period of increased tectonic activity along the Marathon fold belt. As a result, basinal sediments were compacted and the deep sea became anoxic. Broad carbonate shelves growing along the margins of the basins produced organisms whose remains were preserved in the anoxic depths of the sea.

Stage Three: 'Basin Phase,' Permian (299-252 ma.)

-Stage three is defined by rapid synorogenic filling of the Delaware and Midland basins occurred due to fluvial siliciclastic sediments and the development of extensive reef-fringed carbonate and evaporite platforms. Shelves proceeded until all that remained was a small depositional center in the Delaware basin. This resulted in the accumulation of turbidites, over 8,000 feet in thickness. The turbidite accumulation compressed the underlying formations and caused both the Central Basin Platform and the Diablo Platform to be squeezed upward an additional several thousand feet. Finally, as the Permian Sea was isolated and evaporation far exceeded inflow, evaporites filled the remaining basin and the surrounding shelves.

Early Permian (Wolfcampian to Leonardian) –

The rate of subsidence reduced greatly during this period, as well as the rate of sedimentation. Erosion occurred, creating an unconformity, onto which deposits of largely carbonate, shale and fine-grained sandstone were deposited. The eastern shelf of the Midland Basin became completely capped in bedded carbonate deposits and developed a distinct rimmed margin. Circulation of sea water became restricted, but channels in the carbonate shelf and the Val Verde Basin to the south allowed for ample circulation of aerated sea water which aided organics production. Meanwhile, the broad shelves located north, west and east of the Delaware Basin were sites of restricted lagoons in which evaporates deposited.

Middle Permian (Guadalupian) –

Subsidence slowed even further through the Guadalupian. The Midland and Delaware basins were principally sites of siliciclastic accumulation. The shelves were sites of carbonate deposition. During the Middle Guadalupian, the Central Basin Platform and east ceased to accumulate carbonates and became sites of sandstone, anhydrite and halite deposition. Deposits within the Delaware Basin were largely terrestrial sourced clastics. Carbonate deposition ceased as reefs reached sea-level. The Permian Basin soon became isolated as the southwest strait to the sea was blocked off by reefs. Once the Permian Basin was blocked off from the sea, the little sedimentary accumulations that existed became high in organic content. The Delaware Basin later became a deep evaporite lagoon. Guadalupian sediments reached several thousand feet in thickness.

Late Permian (Ochoan) –

Subsidence has halted. The Permian Basin began compacting, and the Ochoan lagoon expanded eastward and northward, causing 1,500 feet of evaporites to be precipitated on the northern and eastern margins of the Delaware Basin. Late in the Ochoan Epoch, a marine incursion deposited the dolomitic Rustler formation over the Permian Basin. The impermeable Castile evaporite, some 2,000 feet thick, was then deposited over the Delaware Basin.

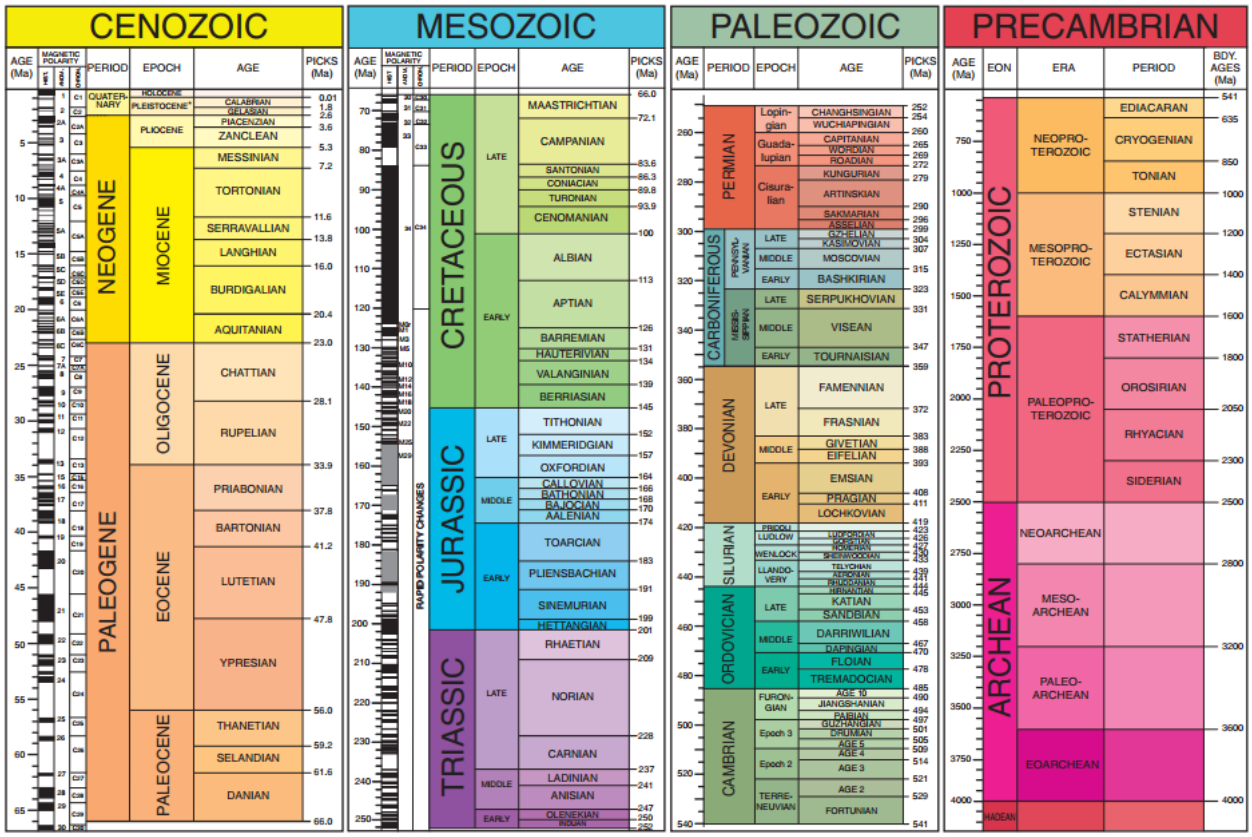

Figure 9 - Geologic Timeline (GSA)

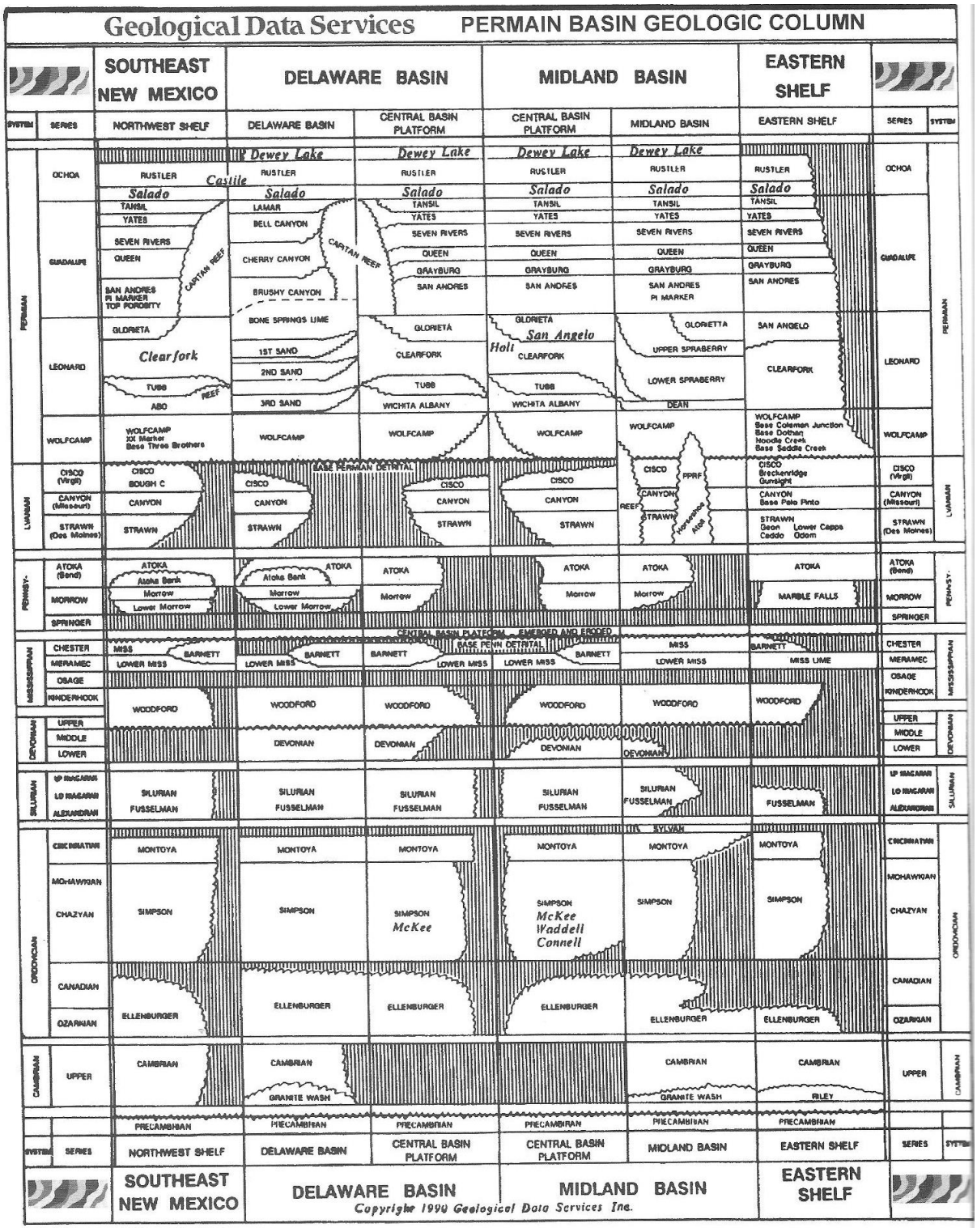

Figure 10 - Permian Basin Geologic Column (WTGS)

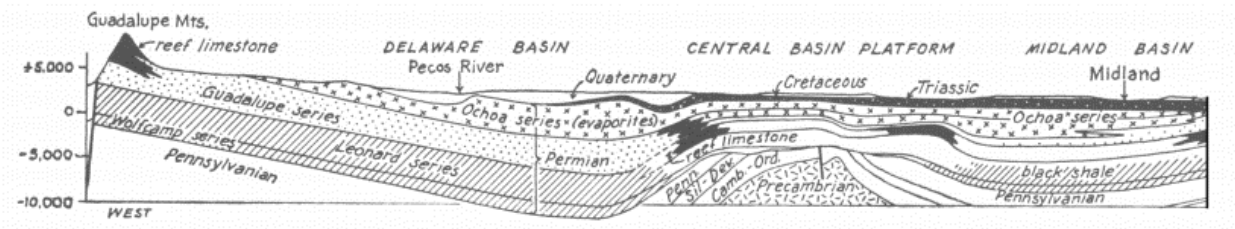

Figure 11 - Permian Basin Cross Section (Urbanczyk)

Conventional Producing Formations:

Central Basin Platform-

Producing formations in the Central Basin Platform contain oil with minor gas accumulations. Hydrocarbons occur in both structural and stratigraphic traps, such as dolomitized shallow-water carbonates, as well as up-dip platform sands and basinal facies. Reservoirs include the Yates, Seven Rivers, Queen, Grayburg, San Andres, Clearfork formations. The CBP accounts for much of the oil production in the Permian Basin.

Source-

Hydrocarbons in the Central Basin Platform are sourced in the organic-rich shaly carbonates and calcareous shale of the Wolfcampian and Leonardian time; to a lesser extent, the Woodford shale of the Late Devonian; and finally, adjoining Pennsylvania and Permian shales located adjacent to the CBP. Hydrocarbons migrated upward, and laterally to present day reservoirs.

Reservoir Info-

Central Basin Platform reservoirs consist of dolomitized carbonates, limestone and fine-grained sandstone. Carbonates were deposited on platforms and along their margins, and reservoir quality was enhanced by the selective dolomitization, dissolution, leaching and fracturing. Reservoirs reach hundreds of feet in thickness, and overall porosity and permeability of twelve percent and eighteen millidarcies. Typical drilling depths are from 1,000 to 10,000 feet. Effective seals were created by impervious dolomite, shaly carbonate, and evaporite facies including anhydrite. Structural and stratigraphic traps are associated with facies changes and impervious sedimentary layers. Also useful to note is that certain formations, such as the San Andres, contain corrosive waters which cause casing leaks if not properly isolated by cement.

Midland Basin & Eastern Shelf-

Producing formations in this region contain oil with minor gas accumulations. Hydrocarbons occur in restricted carbonate platform sedimentary rocks, reefs and siliciclastics. Reservoirs include, but are not limited to, the Yates, Seven Rivers, Queen, Grayburg, San Andres, Clearfork, Spraberry, and

Horseshoe Atoll formations. This region holds the highest oil producing fields in the Permian Basin, including the Slaughter, Wasson and Spraberry.

Source-

Hydrocarbons are sourced in the organic-rich shaly carbonates and calcareous shale of the Permian and Wolfcampian periods (SEPM STRATA).

Reservoir Info-

Oil and gas has been found in zones from every period, from Cambrian through Permian, and in most every known type of subsurface trap. Two of the largest accumulations of hydrocarbons are located in the Horseshoe Atoll and Spraberry trend. Horseshoe Atoll is an accumulation of fossiliferous limestone deposited during the Pennsylvanian through Early Permian period in the northern part of the Midland Basin, and reaches thicknesses of 3,000 feet. The limestone consists of the Strawn, Canyon and Cisco formations, overlain by Wolfcamp sandstone and shale of terrigenous origin. The name is derived from the horseshoe shape of the formation, ninety miles across, seventy miles from north to south, and length of approximately 200 miles. The crest of the atoll is comprised of irregularly shaped hills and depressions, to which oil migrated and was trapped in the porous limestone. The atoll is located at 6,100 to 9,900 feet in depth. The Spraberry trend is a fractured permeability trap on a homoclinal fold about 150 miles in length and thirty-five miles wide. Oil production is continuous along the entire length of the Spraberry. The Spraberry and Dean formations are made up of sand, found in submarine fan systems covering the entire basin. Hydrocarbons are trapped by up-dip pinchouts and facies changes located at depths of 5,100 to 8,300 feet. The sand formations are tightly packed and cemented, resulting in low porosity and average recovery efficiency of fifteen percent (Vertrees).

Delaware Basin & Northwestern Shelf-

The Delaware basin is much deeper than the Midland Basin, which resulted in thin, tightly packed sandstone formations. The greater burial depth of sediments means that there is greater thermal maturity and much deeper reservoirs. Hydrocarbons have therefore developed into natural gas.

Source-

Source rocks are organic-rich basinal shales of Permian age. The low porosity and permeability of tight formations suggests that hydrocarbons were generated from source rock in or nearby the reservoirs, and migration distances were short.

Reservoir Info-

Pay formations are comprised of sandstone, interbedded or laminated with limestone, dolomite and organic rich shale. Formations include Rustler, Yates, Queen, Bone Springs, Avalon, Wolfcamp, Woodford, Barnett and Ellenburger. Much of the Delaware Basin reserves are unconventional. Conventional drilling depths range from 2,000 to 11,000 feet. Unconventional reserves, such as the Ellenburger, have been produced down to approximately 21,000 feet. Traps are mainly stratigraphic. The Delaware Basin plays consist of multiple stacked reservoirs, reaching 3,000 to 3,500 feet in thickness.

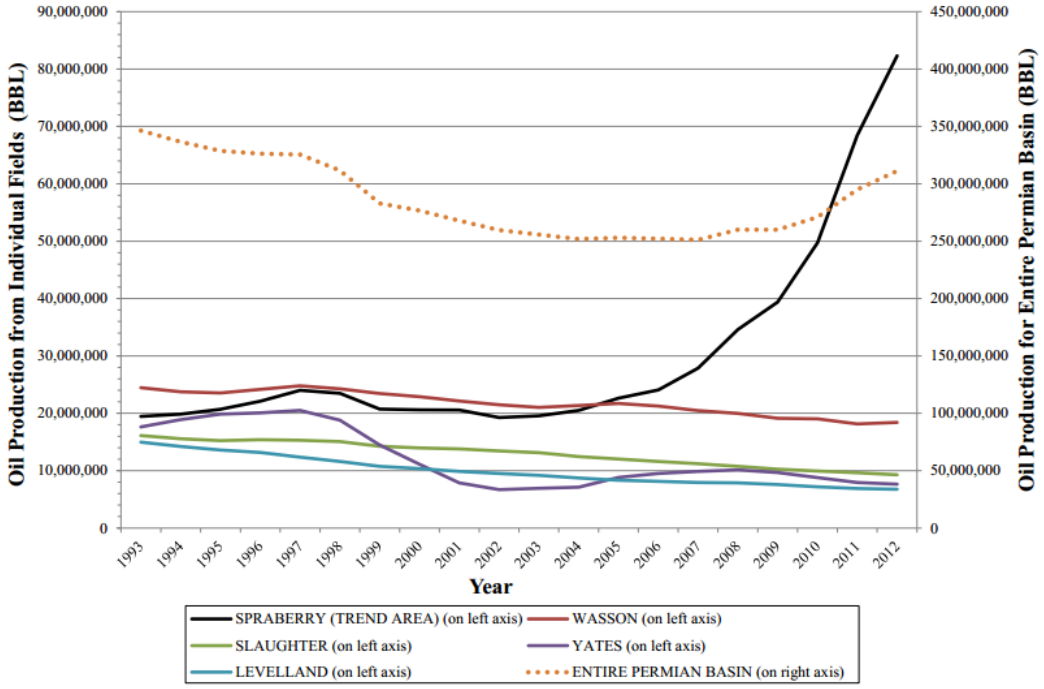

Figure 12 - Yearly Production for Top 10 Current Largest Permian Basin Fields, Part 1/2 (RRC)

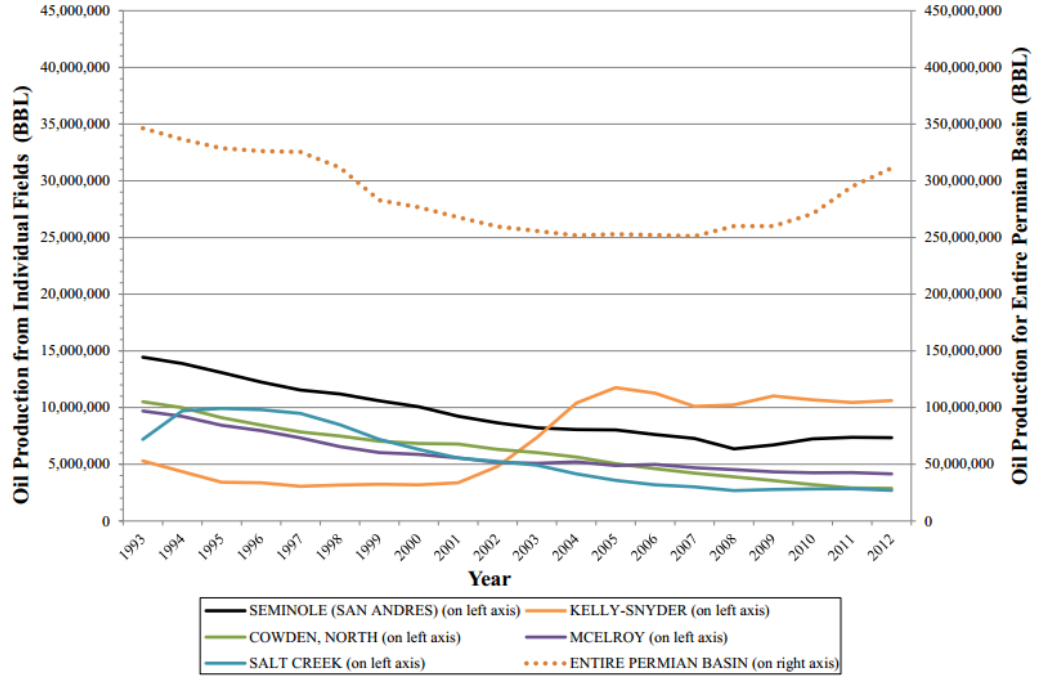

Figure 13 - Yearly Production for Top 10 Current Largest Permian Basin Fields, Part 2/2 (RRC)

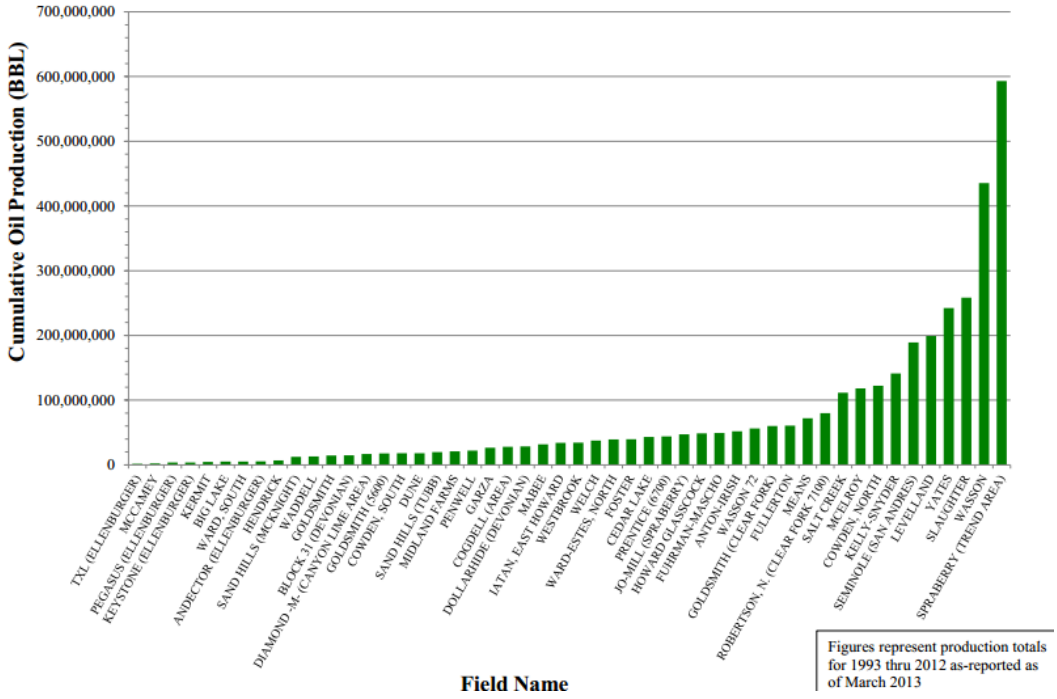

Figure 14 - Top 50 current highest producing Permian Basin oil fields since 1993 (RRC)

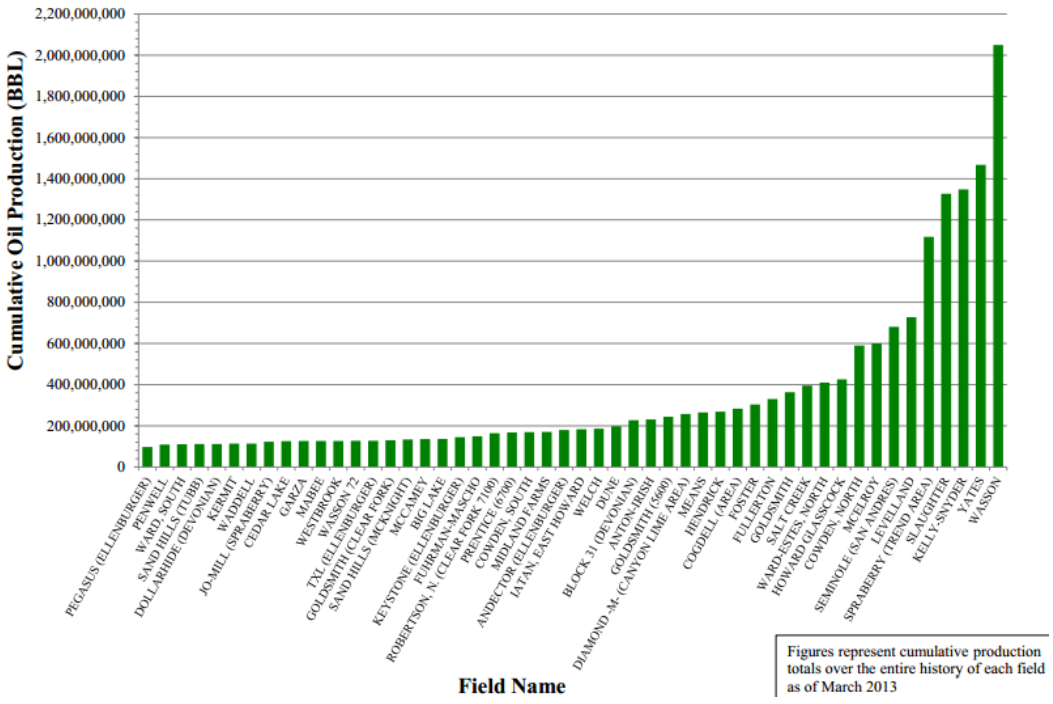

Figure 15 - Top 50 highest producing Permian Basin oil fields, cumulative historical total (RRC)

Unconventional Producing Formations:

Midland Basin: Wolfcamp Oil Shale & Cline Shale

The wolfcamp oil shale, located in the Midland Basin and Central Basin Platform, has been drilled extensively via commingled vertical wells. These plays have commingled the Spraberry and Clearfork formations with the Wolfcamp, giving rise to the names Wolfberry, and Wolffork. The Wolfcamp is Early Permian (Wolfcampian) in age, is located below highly productive formations, and as a result was only drilled into in order to supplement existing production. Thus, extensive exploration did not take place until fairly recently; in conjunction with economically justified crude prices, enhanced oil recovery practices, and the spread of horizontal drilling and 3D seismic mapping (shale experts).

The Wolfcamp formation is typically broken down into four units, A, B, C & D from top to bottom. All of the units are targets for horizontal completions, the most productive being the Wolfcamp A, B, & D units. The hydraulic fracture orientation of the Midland Wolfcamp is generally in the east-west direction, in accordance with the tectonic origins of the basin (Friedrich).

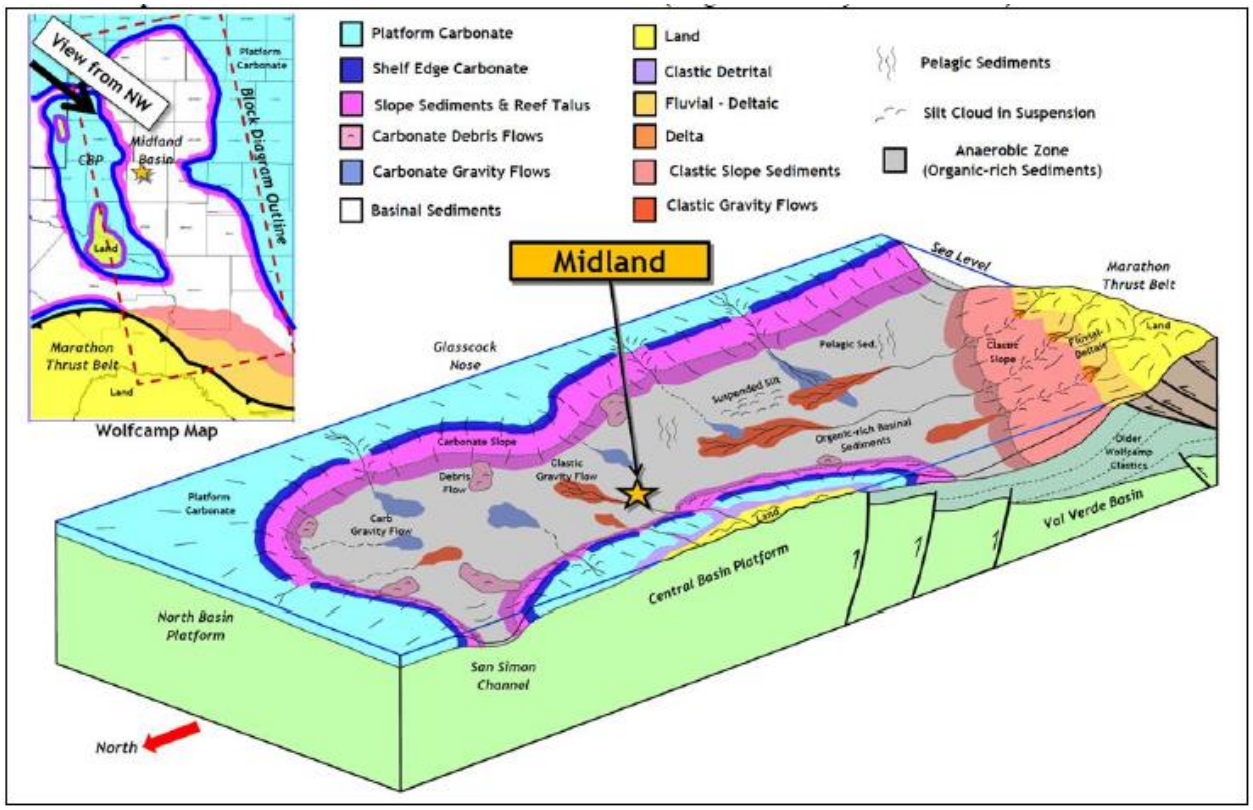

Figure 16 - This block diagram models the distributions of gravity and debris flows and the organic rich basin plain sediments from which the Wolfcamp A and B Facies in the Midland Basin of West Texas originate (Deen)

Table 3 - Midland Basin Wolfcamp Formation Information (Shale Experts)

Age:	Permian
Formation	
Basin:	Midland
Vertical Depth (ft):	5,500 – 10,000
Thickness (ft):	600 – 1100
Porosity (%):	4 – 12
Pressure (PSI,ft):	0.60 – 0.70
Well Information	
Avg. Well Cost (mil):	7.5
Avg.-Lateral (ft):	6500
Avg –EUR(Mboe):	500
OOIP(MMBO):	50 – 100

The Cline shale is located on the eastern edge of the Midland Basin, extending onto the Eastern Shelf. It is an area approximately 140 miles from north to south and 70 miles wide. Cline shale is Late Pennsylvanian in age, and produces oil and natural gas liquids (NGL). The formation is comprised of nearly the entire interval between the Strawn and Wolfcamp D formations (shale experts).

Table 4 - Midland Basin Cline Formation Information (Shale Experts)

Age:	Pennsylvanian
Formation	
Basin:	Midland
Vertical Depth:	9000 - 9500
Thickness (ft):	200 - 350
Thermal Maturity:	0.85 - 1.1

Porosity(%):	5.0 - 12.0
Pressure (PSI,ft):	0.55 - 0.65
Well Information	
OOIP(MMBO):	30,000

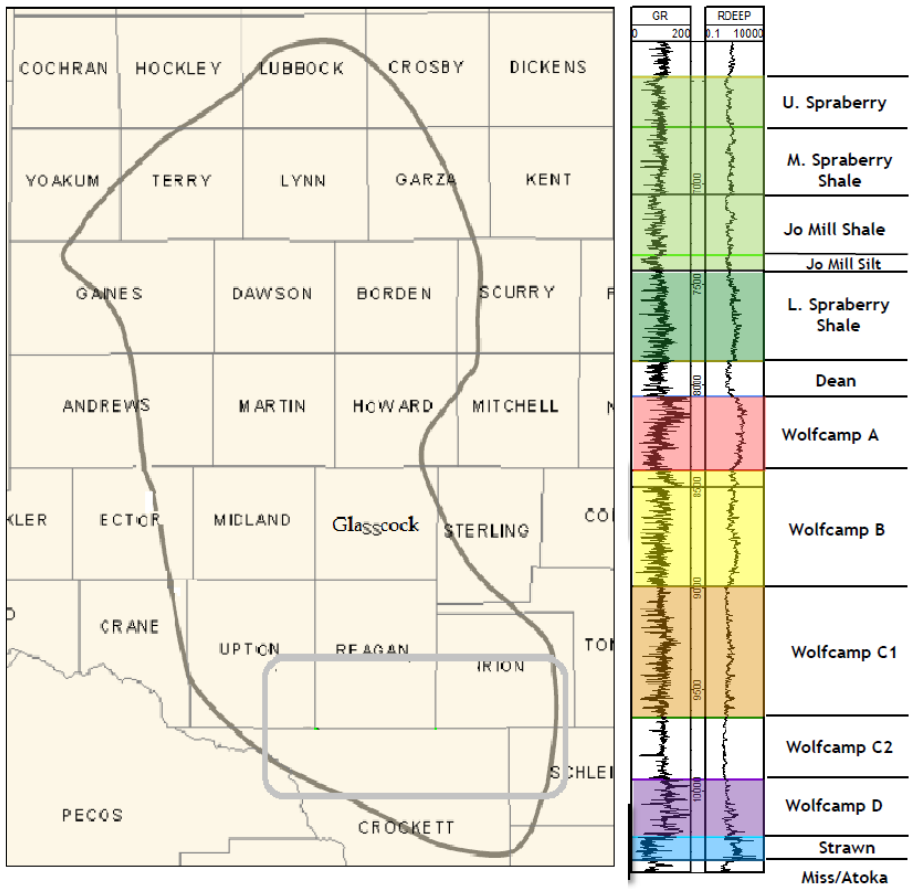

Figure 17 - Typical log response for Midland Basin Lower Permian period (Shale Experts)

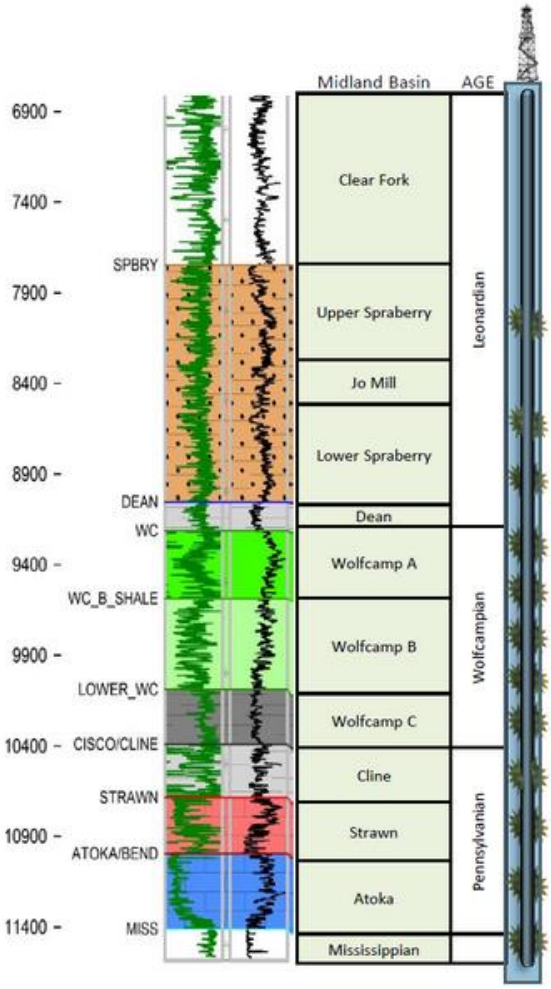

Figure 18 - Typical log response for Midland Basin Lower Permian period (Shale Experts)

Delaware Basin: Wolfcamp & Avalon Shale

The Delaware Wolfcamp shale lies beneath the conventional gas producing sandstone, Bone Spring formation, and is of Wolfcampian age. It is approximately 2,000 feet thick, and produces better further to the north, where the formation is shallower. The Delaware Wolfcamp is often commingled with the Bone Spring formation, giving rise to the term Wolfbone. Development of the Wolfcamp formation is largely horizontal. Production is roughly 60 percent crude, 20 percent wet gas and 20 percent dry gas.

The Avalon shale is located in the upper portion of the Bone Spring formation, sandwiched between the 1st Bone Spring carbonate above, and the 1st Bone Spring sandstone below. It is Middle Permian (Leonardian) in age. The center of operations in the Avalon shale is located just north of the Texas-New Mexico border (shale experts).

Table 5 - Delaware Basin Avalon Formation Information (Shale Experts)

Formation	
Basin:	Delaware Basin
Vertical Depth:	6,500 - 9,000
Thickness (ft):	500
Porosity(%):	13
Well Information	
Avg Well Cost:	6.2
Avg-Lateral (ft):	6000
Avg -EUR(Mboe):	450

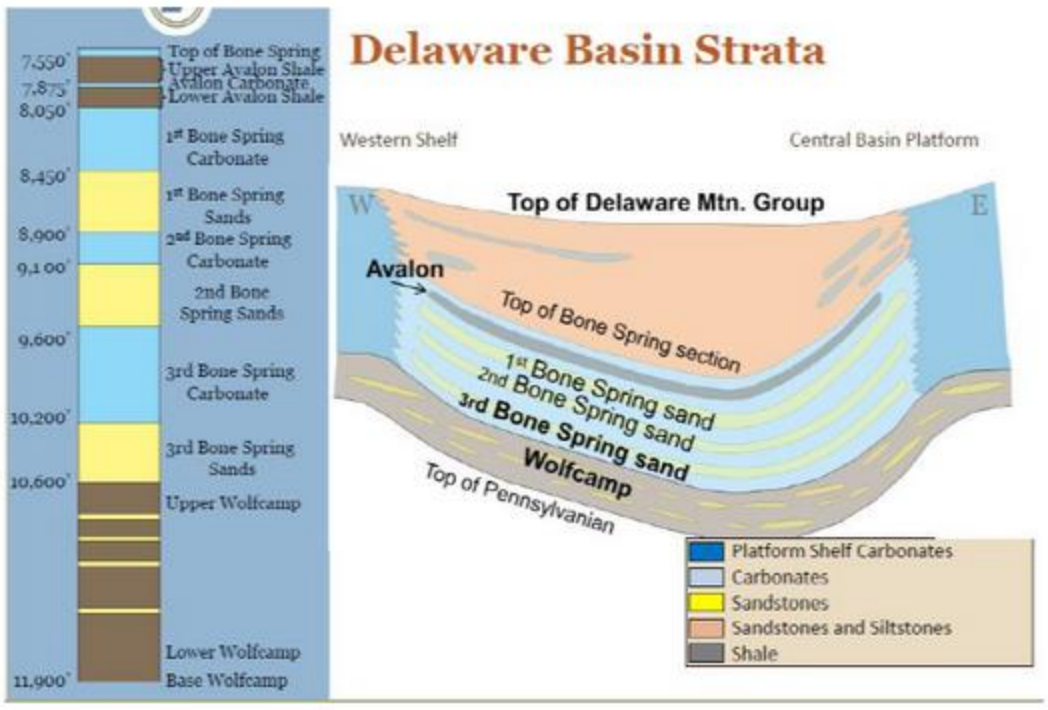

Figure 19 - Delaware Basin Avalon Stratigraphic Map (Shale Experts)

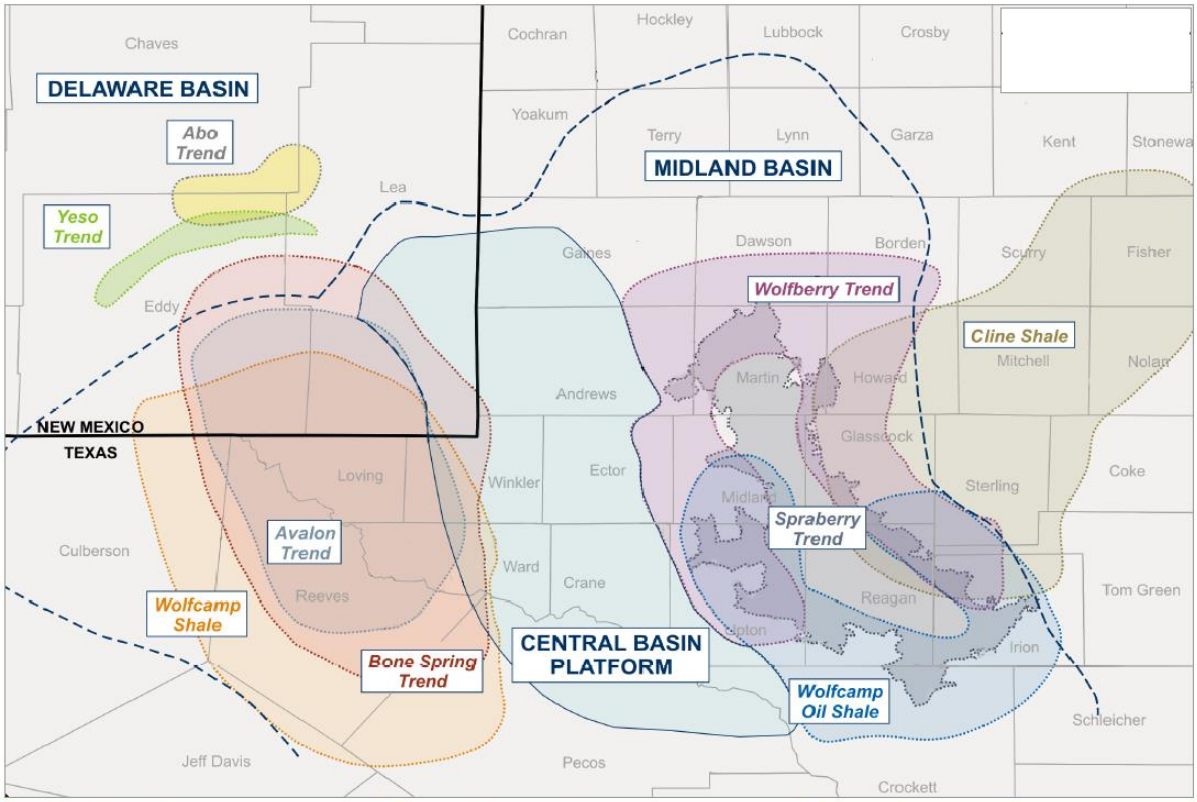

PERIOD	SERIES	DELAWARE BASIN FORMATION
GUADALAUPE	DELAWARE GROUP	LAMAR BELL CANYON
		CHERRY CANYON
		BRUSHY CANYON
LEONARD		UPPER AVALON SHALE
		LOWER AVALON SHALE
		1ST BONE SPRING
		2ND BONE SPRING
		3RD BONE SPRING
WOLFCAMP		WOLFCAMP
PENN		PENNSYLVANIAN

PERIOD	SERIES	CENTRAL PLATFORM FORMATION
GUADALAUPE	WHITE-HORSE	TANSILL
		YATES
		7 RIVERS
		QUEEN
		GRAYBURG
	WARD	SAN ANDRES
		GLORIETA
LEONARD	YESO	PADDOCK
		BLINEBRY
		TUBB
		DRINKARD
	ABO	
WOLFCAMP	WOLFCAMP	HUECO
		BURSUM
PENN	PENNSYLVANIAN	

PERIOD	SERIES	MIDLAND BASIN FORMATION
GUADALAUPE	WHITE-HORSE	TANSILL
		YATES
		7 RIVERS
		QUEEN
		GRAYBURG
	WARD	SAN ANDRES
		GLORIETA
LEONARD	CLEAR FORK	UPPER LEONARD
		UPPER SPRABERRY
		LOWER SPRABERRY
		DEAN
WOLFCAMP		WOLFCAMP
PENN		PENNSYLVANIAN

Figure 20 - Unconventional Formations of the Permian Basin (Shale Experts)

Case Study of the Permian Wolfcamp Formation

The purpose of the following case study was to evaluate the production potential of an emerging unconventional formation in the Permian Basin. The logs provided for this study are listed in the appendix. The evaluated well is located in an undisclosed field in the Midland Basin, located in West Texas. The study formation is an oil bearing shale in the Wolfcamp, units A, B, & C.

Results (Tabular Form):

Table 6 - Case study results, tabular format

RESULTS - Table 1		
OOIP Total in Pay	9,150,392	stb
OOIP by Formation		
Wolfcamp _ - <8040'	885,877	stb
Wolfcamp A - 8040'-8350'	4,710,468	stb
Wolfcamp B - 8350'-8850'	3,339,927	stb
Wolfcamp C - >8850'	214,121	stb
Recoverable OOIP (3% Recovery)		
Wolfcamp _ - <8040'	0	stb
Wolfcamp A - 8040'-8350'	141,314	stb
Wolfcamp B - 8350'-8850'	100,198	stb
Wolfcamp C - >8850'	0	stb
Total Recoverable OOIP	241,512	stb
Pay Criteria		
Avg. k in Pay	265	nD
eff. Porosity avg. in Pay	0.067	V/V
Swe Avg. in Pay	0.466	V/V
Maturity Index Avg.	7	
TOC Avg. - Schmoker	3.71	wt. %
TOC Avg. - Passey	1.69	wt. %
Vitrinite Reflectance Avg.	0.82	%
Pay Zone Thickness by Formation		
Wolfcamp _ - <8040'	17.5	ft
Wolfcamp A - 8040'-8350'	91.5	ft
Wolfcamp B - 8350'-8850'	70.5	ft
Wolfcamp C - >8850'	4	ft
Pay Thickness Total	183.5	ft
Frackable Pay Thickness by Formation		
Wolfcamp _ - <8040'	17.5	ft

Wolfcamp A - 8040'-8350'	91	ft
Wolfcamp B - 8350'-8850'	70	ft
Wolfcamp C - >8850'	4	ft
Total Frackable Pay	182.5	ft
Total Frackable Thickness	840	ft

Picks & Cutoffs (Tabular Form):

Table 7 - Case study picks & cutoffs, tabular format

PICKS & CUTOFFS - Table 2		
Rw	0.035	Ω-m
GRsh	150	API
Rbaseline	100	Ω-m
dtbaseline	56	µsec/ft
Reservoir Parameters		
ka	100	nD
Ro Oil	0.6-1.0	%
TOC	1-10	wt%
Vclay,max - Illite	40	%
Vclay,max - Smectite	4	%
Maturity Index Parameters		
Swe	0.75	V/V
ϕD	0.09	V/V
Frackability Parameters		
Brittleness Coeff.	>44	
σ_{hmin}	5000	psi
µ	0.25	
E	3.0E+06	psi

Case Study Procedure:

1.) CALCULATION of TOTAL POROSITY [Φtotal]:

Schmoker TOC Equation:

$$TOC = \frac{156.956}{\rho_b} - 58.271$$

Passey TOC dlogR Method:

$$TOC = \Delta\log(R) * 10^{(2.297 - 0.1688 * LOM)} \qquad where: LOM = 7\ for\ a\ mature\ oil\ source.$$

$$\Delta\log(R) = \log\left(\frac{R}{R_{baseline}}\right) + 0.02 * (\Delta t - \Delta t_{baseline})$$

$$where: \quad R_{baseline} = 100\ \Omega m, \ \ and \quad \Delta t_{baseline} = 56\ \frac{\mu sec}{ft}, \qquad taken\ from\ logs.$$

Volume of Kerogen:

$$V_{ke} = \frac{TOC * \rho_b * K_v}{\rho_{kerogen}} / 100 \qquad Given: K_v = 1.2,\ \rho_{kerogen} = 1.5$$

Normalized Volumes:

$$V_{cl} + V_{qtz} + V_{cal} + V_{pyr} + V_{ke} = TOTAL$$

$$\frac{V_{cl}}{TOTAL}, \ \frac{V_{qtz}}{TOTAL}, \ \frac{V_{cal}}{TOTAL}, \ \frac{V_{pyr}}{TOTAL}, \ \frac{V_{ke}}{TOTAL}$$

Determine ρma:

$$\rho_{ma} = (2.71 * V_{cl}) + \left(2.65 * V_{qtz}\right) + (2.71 * V_{cal}) + \left(5 * V_{pyr}\right) + (1.5 * V_{ke})$$

Dry density of Illite = 2.71

Total Porosity:

$$\varphi_{total} = \frac{(\rho_{ma} - \rho_b)}{(\rho_{ma} - \rho_f)}$$

$$Where:\ \rho_f = 1.1 * S_w + \rho_{hc}(1 - S_w) \qquad Use\ S_w\ instead\ of\ S_{xo}\ because\ no\ flushed\ zone.$$

$$Given: S_w = 0.2,\ \ \rho_{hc} = 0.85\ \frac{g}{cm^3},\ Oil$$

2.) DETERMINE EFFECTIVE POROSITY [Φe]:

$$\varphi_e = \varphi_{total} - CBW$$

$$CBW = V_{cl} * \varphi_{clay} \qquad given: \varphi_{clay} = 0.10\ (Illite)$$ provided for formation.

3.) DETERMINE ORGANOPOROSITY [Φom]:

$$\varphi_{om} = \varphi_{ke} * V_{ke} \qquad given:\ \varphi_{ke} = 0.3$$

4.) DETERMINE MINERAL MATRIX POROSITY [Φmm]:

$$\varphi_{mm} = \varphi_e - \varphi_{om}$$

5.) DETERMINE MATURIY INDEX [MI] Zhao & others, 2007

This equation only applies if $S_{we} \leq 75\%\ and\ \varphi_{Dls} \geq 9\%$.

$$MI = \sum \frac{1}{N * \varphi_{nls} * \sqrt{1 - S_{we}}} \qquad where: \Sigma = 1\ to\ N$$

$$S_{we} = \sqrt{\frac{R_w(\frac{1}{\varphi_e^2})}{R_{sh}}}$$

6.) DETERMINATION of OOIP (stb) [Φom]:

$$OOIP(stb) = \Sigma \frac{7758 * h(ft) * A(ac) * \varphi_{oil}}{BOI} \qquad given:\ A = 160\ acres$$

$$\varphi_{oil(om)} = \varphi_{om}(1.0 - S_w) \qquad where: S_w = 0$$

$$[MI < 6.0\%\ R_o < 8.0,\ BOI = 1.2\ low\ shrinkage\ oil]$$

$$[MI > 6.0\%\ R_o > 8.0,\ BOI = 1.4\ high\ shrinkage\ oil]$$

7.) DETERMINATION of OOIP (stb) [Φmm]:

$$OOIP(stb) = \Sigma \frac{7758 * h(ft) * A(ac) * \varphi_{oil}}{BOI} \qquad given:\ A = 160\ acres$$

$$\varphi_{oil(mm)} = \varphi_{mm}(1.0 - S_w)$$

$$S_w = \sqrt{\frac{1 * R_w}{\varphi^2 * R_t}} \qquad (Archie's\ eq.) \qquad where: \varphi = \varphi_{total} - \varphi_{om}$$

$[MI < 6.0\%\ R_o < 8.0,\ BOI = 1.2\ low\ shrinkage\ oil]$

$[MI > 6.0\%\ R_o > 8.0,\ BOI = 1.4\ high\ shrinkage\ oil]$

8.) CALCULATE PERMEABILITY [ka] Rick Lewis, Schlumberger:

$k_a = (10.8 * \varphi_{oil} - 0.256) * 10^3 \quad (nanodarcies, nD)$

$\varphi_{oil} = \varphi_{oil(mm)} + \varphi_{oil(om)} \quad where: reservoir > 100nD$

9.) ROCK GEOMECHANICS:

Poisson's Ratio [μ]

$\mu = \frac{0.5*\left(\frac{\Delta t_S}{\Delta t_C}\right)^2 - 1}{\left(\frac{\Delta t_S}{\Delta t_C}\right)^2 - 1} \qquad \mu \leq 0.25,\ stiff\ rock.$

Young's Modulus [E]

$E = 2 * 1.34 * 10^{10} * \frac{\rho_b}{\Delta t_s^2} * (1 + \mu) \qquad E \geq 3 * 10^6, along\ with\ \mu \leq 0.25, enables\ fracturing.$

Brittleness Coefficient [BC] Bateman, after Mullen, OLAFE:

$BC = 50 * \left(\frac{E-1}{7} + \frac{0.4-\mu}{0.25}\right) \qquad BC > 44,\ corresponds\ to\ frackable\ rock.$

Minimum Closure Stress [σHmin psi]:

$$\sigma_{hmin} = \frac{\mu}{1-\mu} * \left(\sigma_v - \left(X * P_p\right)\right) + \left(X * P_p\right) \qquad \sigma_{hmin} \leq 5000psi, fracture\ retention.$$

$$P_p = depth * 0.43\,\frac{psi}{ft} \qquad (pore\ pressure)$$

$$\sigma_v = depth * 1.08\ \frac{psi}{ft} \qquad (vertical\ stress)$$

$$X = 1.0 \quad (poroelastic\ constant)$$

$$stress\ gradient = \frac{\sigma_{hmin}}{depth}$$

Mineral Brittleness Index [MBI] Wang & Gale, 2009:

$$MBI = \frac{V_{qtz}+V_{cal}}{V_{qtz}+V_{cal}+V_{clay}+V_{ke}}$$

10.) MOVEABLE OIL:

Mud Filtrate Resistivity [Rmfa]:

$$R_{mfa} = R_{xo} * \varphi_{total}^2$$

Invaded Zone Saturation [Sxo]:

$$S_{xo} = \sqrt{\frac{1*R_{mf}}{\varphi_{total}^2*R_{xo}}} \qquad where:\ R_{mf}\ \ is\ determined\ from\ R_{mfa}\ values$$

It was determined that Sxo is not greater than Sw, therefore there is no moveable oil.

Plots, Logs & Analysis:

(See appendix for logs.)

Mineral Composition:

From the mineral composition log, it can be seen that the Wolfcamp A formation is comprised mainly of carbonate, with low clay percentages, <30%. The volume of kerogen is relatively constant throughout the logged interval. The Wolfcamp B & C formations have higher clay content as well as tight streaks of carbonate contained within mainly sandstone formations. The volume of pyrite was also important in the calculation of matrix density due to the high density, 5 g/cc.

Spectral Gamma Ray & SP:

The spectral gamma ray logs, both with Uranium activity (HSGR) and without Uranium activity (HCGR), show the concentration of organic material via the amount of separation between the two curves. The high API is indicative of illite clay (figure 24). The SP reading provides radiation free lithology information, and varies in accordance with the HCGR log, due to the conductivity of the clay content.

U, Th & K Concentrations:

The elemental gamma ray logs provide insight into the sources of radiation. The relatively high potassium percentages are indicative of illite clay. However, the high thorium concentrations are more typical of smectite or mixed clays. The concentration of uranium shows that there is high organic content throughout the logged interval.

Matrix Identification (MID) Plot:

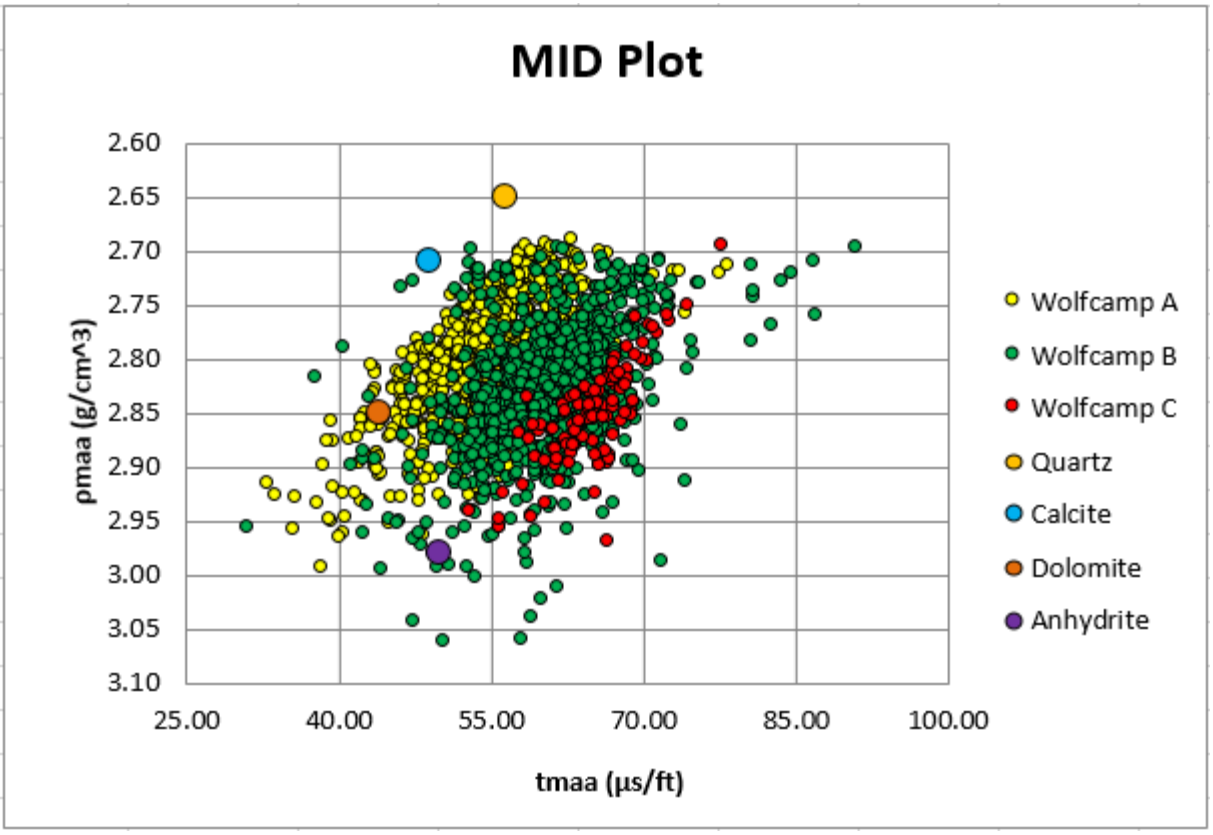

Figure 21 - Matrix Identification (MID) plot of tmaa vs. rhomaa

The MID plot gives an indication of rock type. From the plot it can be seen that the apparent matrix transit time increases with depth. Also, the apparent matrix density appears to increase with depth. The data indicates mixed lithology, tending towards dolomitic concentrations.

U Matrix Lithology:

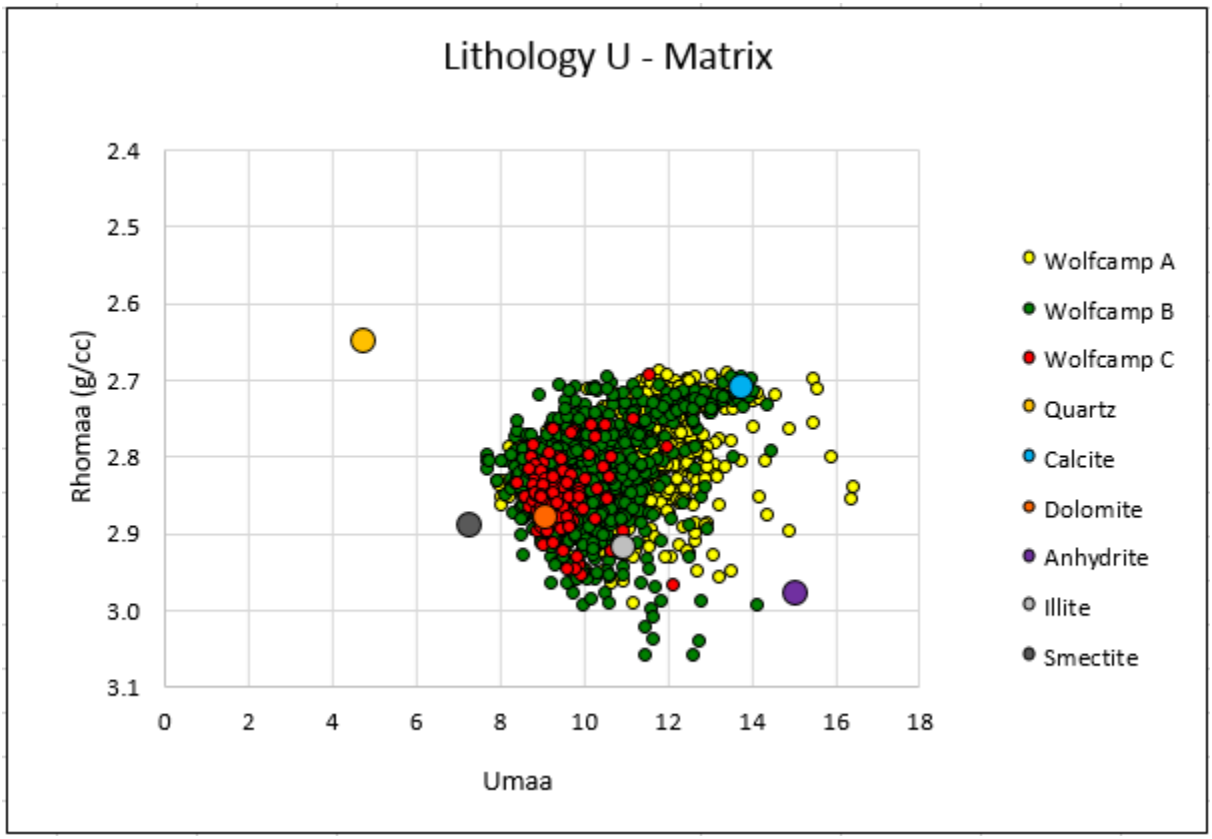

Figure 22 - Lithology U Matrix plot of Umaa vs. Rhomaa

This plot shows the apparent matrix volumetric photoelectric factor, Umaa plotted against apparent matrix density. The plot clearly defines the Wolfcamp formation as varying mainly between dolomite and carbonate, with varying percentages of both sandstone and Illite clay.

Clay Type:

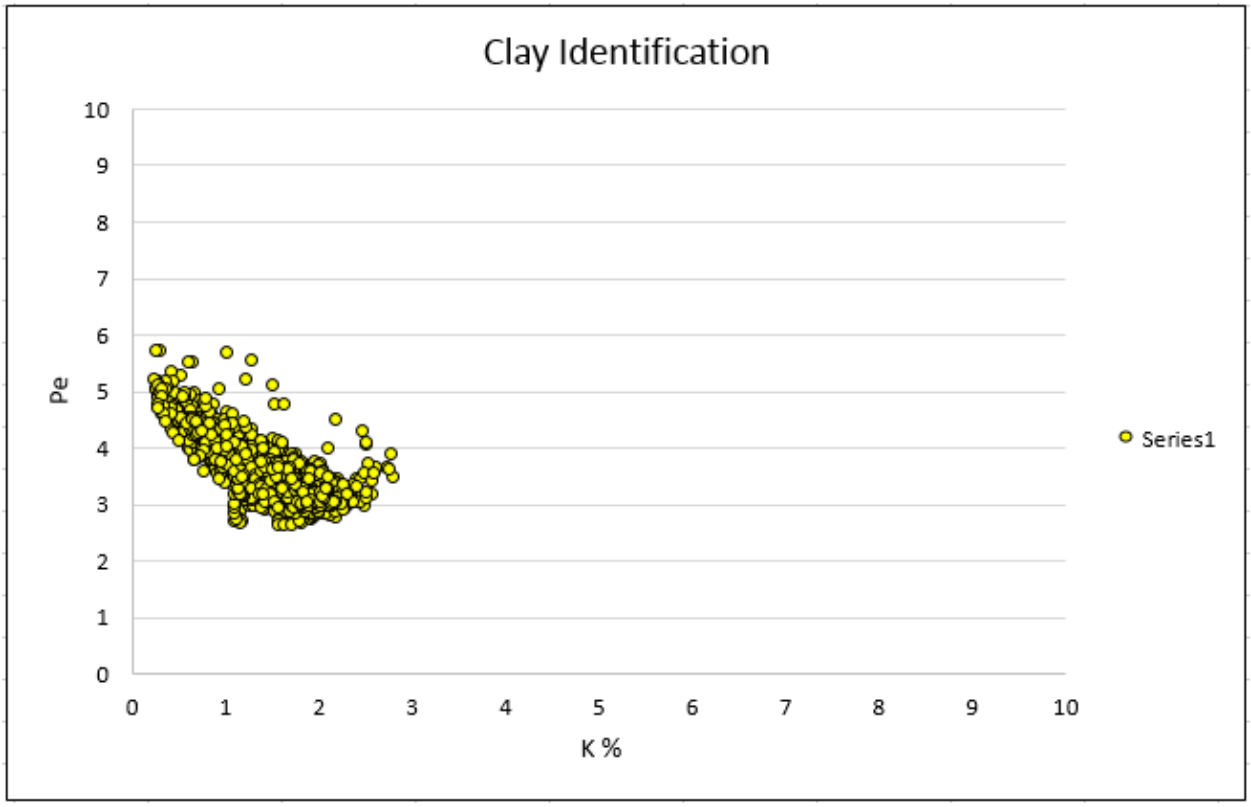

Figure 23 - Clay type plot of Potassium vs. Photoelectric Factor

The plot of Potassium vs. Photoelectric factor is perplexing. The potassium concentration is more in line with that of a smectite clay; however, the Pe values are more indicative of Illite clay. Potassium concentrations of Illite clays should be in the range of 4 to 8 percent. Perhaps there was an error during logging, or the log headings were mixed up with either thorium or uranium readings, or perhaps this is an atypical formation.

Deep & MCFL Resistivity:

The micro-cylindrically focused and deep induction resistivity readings exhibit little separation throughout the logged interval. This indicates little or no invaded zone, in accordance with the expected low porosity and permeability of a tight carbonate/sand stone formation at this depth.

LMS Scaled N-D Porosity & Pe Overlay:

The limestone scaled overlay is more useful in lithology determination than hydrocarbon identification. In the upper portion of the formation and in various tight streaks throughout, where there is little or no separation between logs, the matrix is comprised mainly of limestone. Throughout the rest of the logged interval, the logs have separation, and parallel each other, which is indicative of shale or dolomite. Also, along with the spectral gamma ray logs, the neutron-density porosity readings are indicative of illite clay when compared to values in the below figure, 24.

	Chlorite	Kaolinite	Illite	Montmorillonite
ρ_{ma} g/cc	2.6-2.96	2.6-2.7	2.6-2.9	2.2-2.7
$(\rho_{ma})_{av}$ g/cc	2.79	2.63	2.65	2.53
CEC meq/100 g	10-40	3-15	10-40	80-150
GR (relative)	1	9	100	5
Σ_{ma} cu	25	14	17.2	11.2
P_e	6.33	1.84	3.55	2.3
$(\phi_{Nsh})_{av}$ %	52	37	30	44
$(\phi_{Dsh})_{av}$ %	-7	15	8	32
$\phi_{Nsh} - \phi_{Dsh}$ %	59	22	22	12
ϕ_T %	29.5	26	19	38

Figure 24 - Clay Properties Table (OLAFE)

Sonic Porosity, Bulk Density Overlay:

Sonic tools tend to overlook vugs and fractured porosity because compressional waves will bypass areas of slower travel, such as fluids, by traveling through the matrix. The density logs will however respond to voids in the matrix. Therefore, when overlaid, the two logs will cross over in areas of secondary porosity. The plot shows that there is no secondary porosity.

Passey Method:

For the Passey method to work, the logs must be properly scaled and overlain. The relative scaling is a ratio of -50 µsec/ft per one resistivity cycle. The curves were overlain and baselined in a non-source rock. Non-source and non-reservoir zones tend to have overlying porosity and resistivity curves, and is where the baseline values are taken from. In this study, the baseline values were taken from 8684.5'-8687', in a tight streak, where no organic material or hydrocarbons were present. Tight zones can be recognized by short transit times of around 55 µsec/ft. Organic rich intervals were then calculated based on the separation between the two curves (dlogR). From the dlogR values, the total organic carbon (TOC wt%) was calculated. The Passey method indicated lower average TOC levels than did the Schmoker method (1.7 vs. 3.7 wt%, respectively). As illustrated in the figure below, the determination of reservoir and source rock can be made through log interpretation. In general, immature zone

response is due entirely too sonic curve response; mature zones have both sonic and resistivity curve components, and reservoirs tend to exhibit resistivity curve separation mainly due to non-conductive hydrocarbons. From this method, it can be seen that the Wolfcamp A formation is a low porosity reservoir.

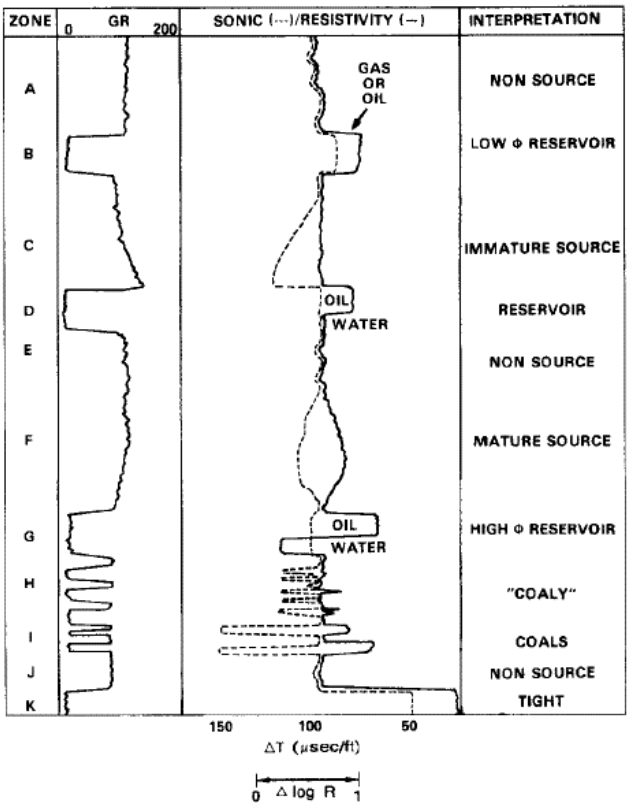

Figure 25 - Passey method interpretation

HCPV:

This log displays stacked area of hydrocarbon pore volume in both the organic and mineral matrix. As is evident in the log, the majority of the oil is located in the organic matrix. This is due to the low effective porosity in the mineral matrix of around 1%; whereas, the porosity in the organic matrix was 2-3%.

Vitrinite Reflectance & Permeability:

For this study, reservoir rock was defined as having at least 100 nD permeability. Vitrinite reflectance data provided a maturation indicator for the upper hydrocarbon bearing zones. The oil window is between vitrinite reflectance values of 0.6-1.0%. The limiting factor for production from this well is permeability in the extremely tight reservoir rock.

Geomechanical Properties:

Based on the lithology, and defining this as a high organic content formation, a Poisson's ratio of 0.25, and a Young's modulus of 3e6 psi were chosen as the limiting criteria for producing hydraulic fractures. From there, it was determined that 840' of the 900' logged section could be readily fractured. This would potentially result in increased production from the fractured segment, not just limited to the existing 100 nD intervals.

Brittleness Coeff. & Closure Stress:

A minimum closure stress of around 5000 psi or less is ideal for maintaining hydraulic fracture width, and therefore conductance. The entire formation is right around 5000 psi, which is in accordance with required geomechanical properties required for hydraulic fracturing. A brittleness coefficient of 44 corresponds to the determined Poisson's and Young's Modulus criteria.

Recommendations:

This reservoir has potential to produce economically due to the shear thickness of oil bearing rock, 840'. Though the reservoir is extremely tight, permeability in the nano-Darcy range, it has good properties for hydraulic fracturing. Based on this study, 840' of the 900' logged can be fractured, including nearly 100% of the pay zone thickness. Therefore, this well could be economically justifiable despite the estimated 3% recovery. As is evident in the table of results, the Wolfcamp zones A & B are the target zones for completion.

Acidizing with HF acid is out of the question in dissolving clays due to the formation of solid precipitants in a carbonate reservoir. Acidizing with an HCl treatment in the carbonate reservoir of the Wolfcamp A formation could be a possible stimulation treatment.

Appendix:

Logs

The following logs were provided for evaluation of the Wolfcamp, A (8040'-8350'), B (8350'-8850'), and C (8850'-8900') formations at an undisclosed well location in the Permian Basin.

DEPT.F	Depth (MD)
AT10.OHMM	AIT-H 10 INVESTIGATION
AT20.OHMM	16 2Ft Vert. Res. 20in D.I.
AT30.OHMM	AIT-H 30 INVESTIGATION
AT60.OHMM	18 2Ft Vert. Res. 60in D.I.
AT90.OHMM	AIT-H 90 INVESTIGATION
DCAL.IN	Differential Caliper {F11.4}
DNPH.CFCF	Delta Thermal Neutron Porosity {F11.4}
DPHZ.CFCF	HRDD Standard Resolution Density Porosity
DSOZ.IN	HRDD Standard Resolution Density Standoff
DTCO.US/F	Delta-T Compressional {F11.4}
DTSM.US/F	Delta-T Shear {F11.4}
DWAL_WALK2.	Dry Weight Fraction Pseudo Aluminum (SpectroLith)
DWCA_WALK2.	Dry Weight Fraction Calcium (SpectroLith)
DWFE_WALK2.	Dry Weight Fraction Iron + 0.14 Aluminum
DWGD_WALK2.PPM	Dry Weight Fraction Gadolinium (SpectroLith)
DWSI_WALK2.	Dry Weight Fraction Silicon (SpectroLith)
DWSU_WALK2.	Dry Weight Fraction Sulfur (SpectroLith)
DWTI_WALK2.	Dry Weight Fraction Titanium (SpectroLith)
ECGR.GAPI	Gamma-Ray {F11.4}
GR.GAPI	Gamma-Ray {F11.4}
HCGR.GAPI	HNGS Computed Gamma Ray (without Uranium) {F11.4}
HDRA.G/C3	HRDD Density Correction {F11.4}
HPRA.	HRDD Photoelectric Factor Correction {F1

HSGR.GAPI	HNGS Standard Gamma Ray (U, K & Th) {F11.4}
HPOT.%	HNGS Formation Potassium Concentration
HTHO.PPM	HNGS Formation Thorium Concentration {F1
HURA.PPM	HNGS Formation Uranium Concentration {F1
HTNP.CFCF	HiRes Thermal Neutron Porosity {F11.4}
HTNP_SAN.CFCF	HiRes Thermal Neutron Porosity (matrix S
ITT.	INTEGRATED TRAVEL TIME MARK
NPHI.CFCF	Thermal Neutron Porosity (Ratio Method)
NPOR.CFCF	Enhanced Thermal Neutron Porosity {F11.4
PEFZ.	HRDD Standard Resolution Formation Photo
PR.	Poisson's Ratio {F11.4}
RHGE_WALK2.G/C3	Matrix Density from Elemental Concentration
RHOZ.G/C3	HRDD Standard Resolution Formation Density
RSOZ.IN	MCFL Standard Resolution Resistivity
RXO8.OHMM	MCFL High Resolution Invaded Zone Resist
RXOZ.OHMM	MCFL Standard Resolution Invaded Zone Re
SP.MV	Spontaneous Potential
SPHI.CFCF	Sonic Porosity {F11.4}
TENS.LBF	Cable Tension {F11.4}
TNPH.CFCF	Thermal Neutron Porosity {F11.4}
WANH_WALK2.	Dry Weight Fraction Anhydrite/Gypsum (SL WA)
WCAR_WALK2.	Dry Weight Fraction Carbonate (SpectroLith WA)
WCLA_WALK2.	Dry Weight Fraction Clay (SpectroLith WA)
WCOA_WALK2.	Dry Weight Fraction Coal (SpectroLith WA)
WEVA_WALK2.	Dry Weight Fraction Salt (SpectroLith WA)
WPYR_WALK2.	Dry Weight Fraction Pyrite (SpectroLith WA)
WQFM_WALK2.	Dry Weight Fraction Quartz+Feldspar+Mica (SL WA)
WSID_WALK2.	Dry Weight Fraction Siderite (SpectroLith WA)

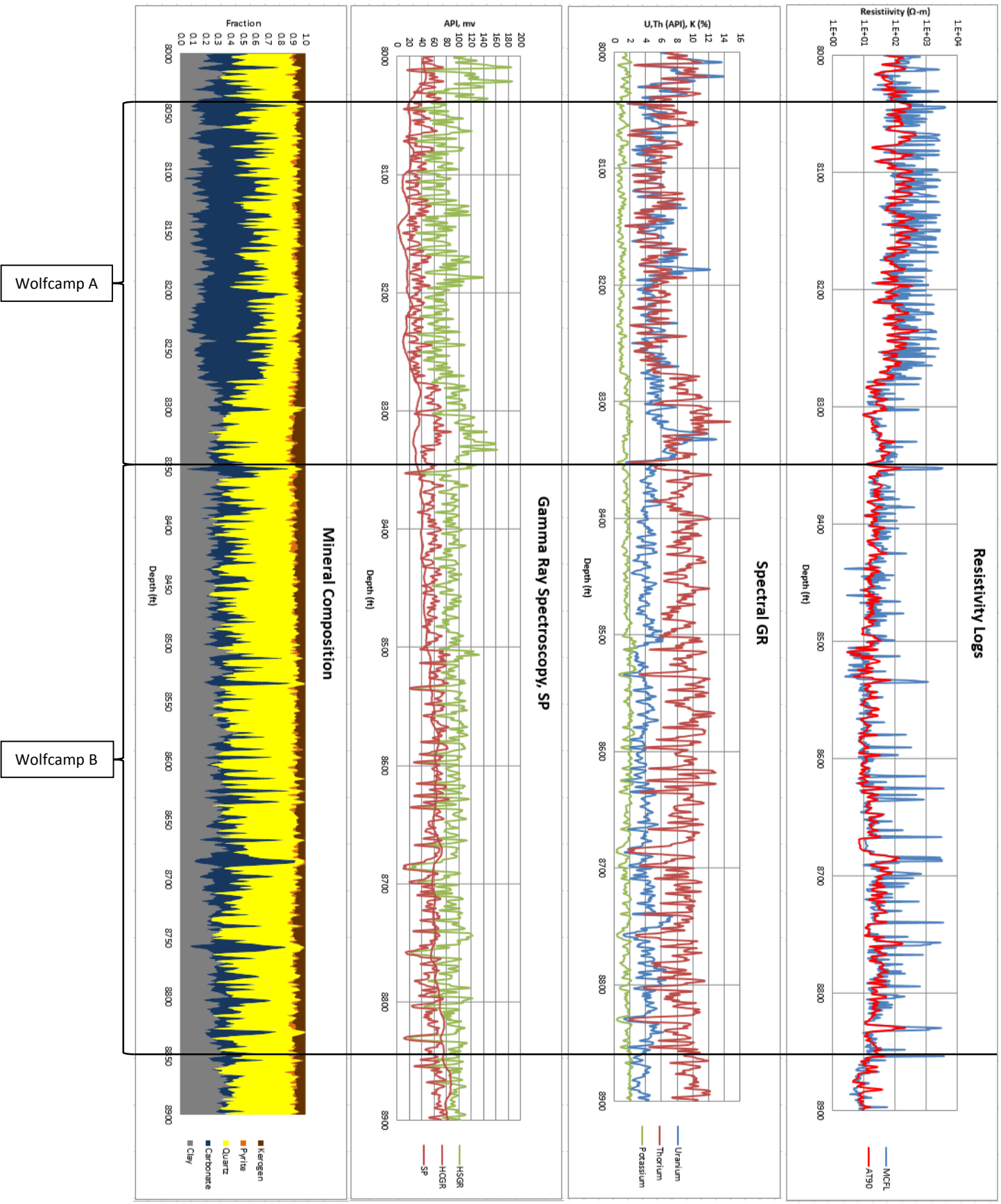
Wolfcamp A
Wolfcamp B
Resistivity Logs
Resistiivity (Ω-m)
1E+04
1E+03
1E+02
1E+01
1E+00
MCFL
AT90
Spectral GR
U,Th (API), K (%)
16
14
12
10
8
6
4
2
0
Uranium
Thorium
Potassium
Gamma Ray Spectroscopy, SP
API, mv
200
180
160
140
120
100
80
60
40
20
0
HSGR
HCGR
SP
Mineral Composition
Fraction
1.0
0.9
0.8
0.7
0.6
0.5
0.4
0.3
0.2
0.1
0.0
Kerogen
Pyrite
Quartz
Carbonate
Clay
Depth (ft)
8000
8050
8100
8150
8200
8250
8300
8350
8400
8450
8500
8550
8600
8650
8700
8750
8800
8850
8900

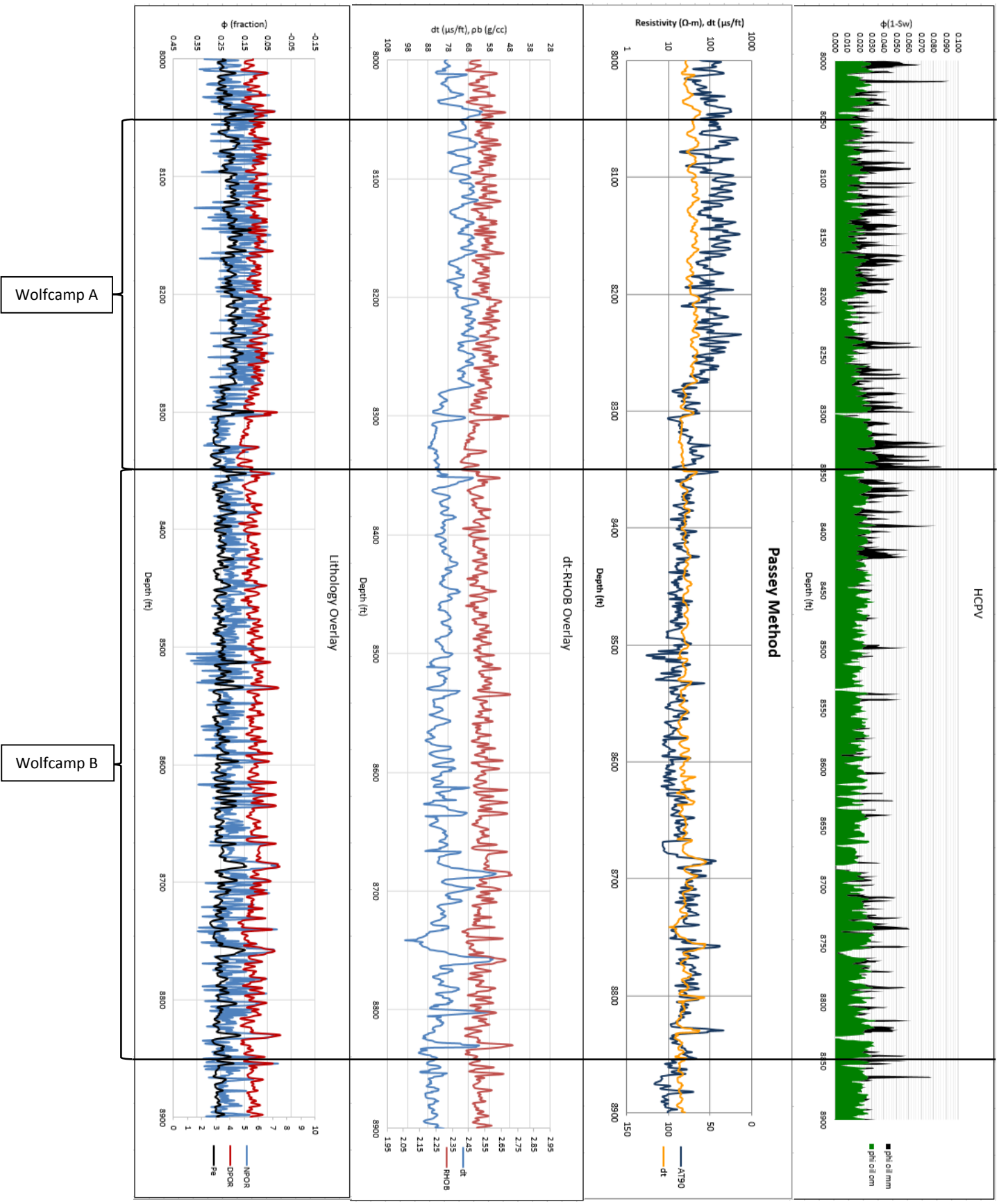
Wolfcamp A
Wolfcamp B
HCPV
ϕ(1-Sw)
phi oil mm
phi oil cm
Passey Method
Resistivity (Ω-m), dt (µs/ft)
AT90
dt
dt-RHOB Overlay
dt (µs/ft), pb (g/cc)
RHOB
dt
Lithology Overlay
ϕ (fraction)
NPOR
DPOR
Pe
Depth (ft)

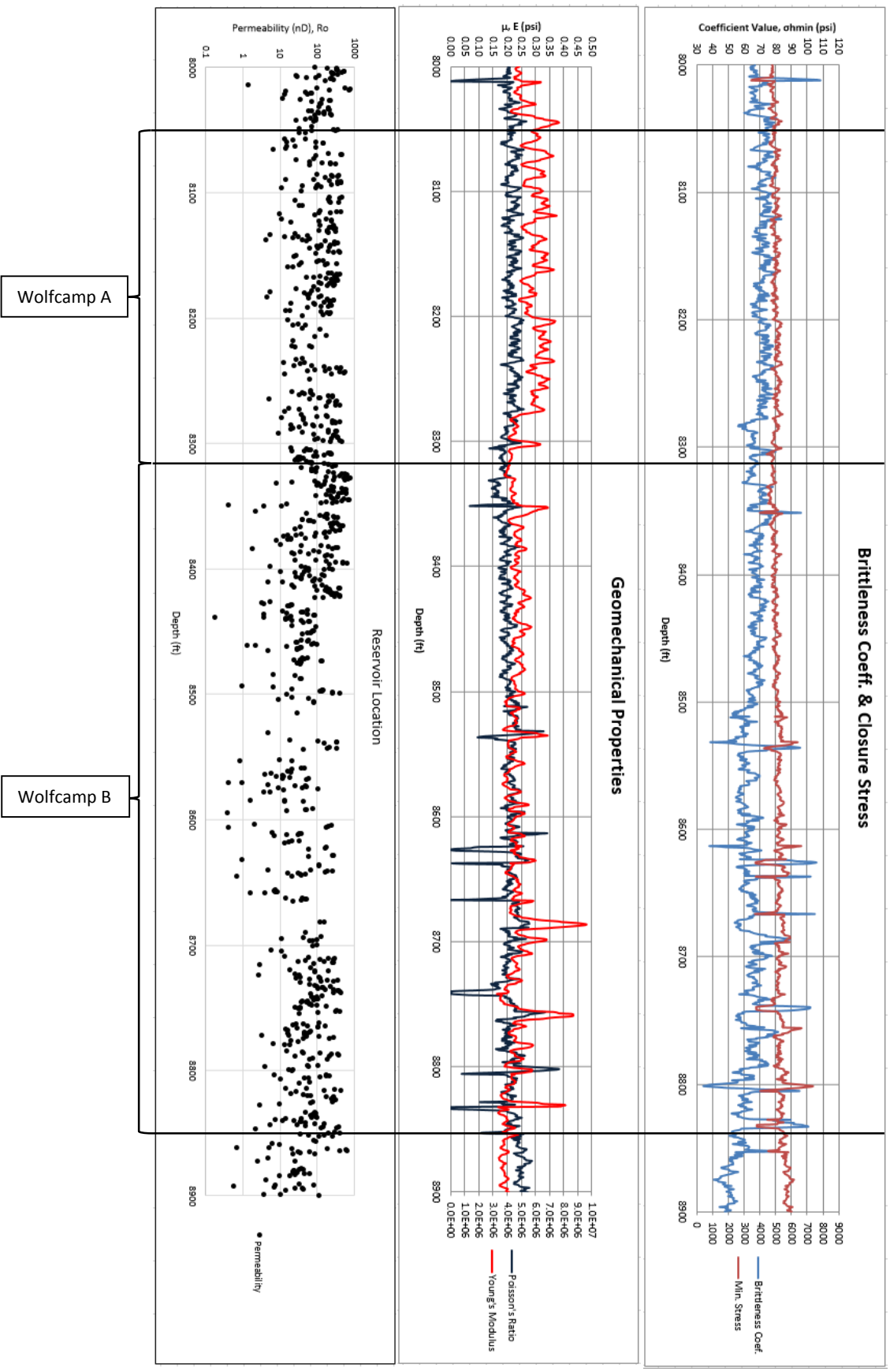
Wolfcamp A
Wolfcamp B
Brittleness Coeff. & Closure Stress
Coefficient Value, σhmin (psi)
Depth (ft)
Brittleness Coef.
Min. Stress
Geomechanical Properties
μ, E (psi)
Depth (ft)
Poisson's Ratio
Young's Modulus
Reservoir Location
Permeability (nD), Ro
Depth (ft)
Permeability

Nomenclature

From the logs listed above, the following values were calculated (**Procedure**) for further evaluation:

(TOC)	Total Organic Carbon (Schmoker)
(V_{xx})	Volumes of clay, quartz, carbonate, pyrite and kerogen
(ρ_{ma})	Matrix density (g/cc)
(φ_{total})	Total Porosity
(CBW)	Clay bound water
(φ_e)	Effective porosity
$(\varphi_{om}, \varphi_{mm})$	Porosity of organic and mineral matrices
(S_{we})	Effective water saturation
(MI)	Maturity Index
(S_w)	Water saturation (Archie)
$(\varphi_{oil(om)}, \varphi_{oil(mm)})$	Oil filled porosity, organic and mineral matrix
$(OOIP)$	Oil in place (stb)
(k_a)	Permeability (nD)
(S_{xo})	Invaded zone saturation
(E)	Young's Modulus (psi*10^6)
(MBI)	Mineral Brittleness Index
(BC)	Brittleness Coefficient
(σ_{hmin})	Minimum Closure Stress

References:

Cimarex (2005, Sep. 28). Cimarex Energy Saya Gas Production Remains Shut-in. http://www.rigzone.com/news/oil_gas/a/25612/Cimarex_Energy_Says_Gas_Production_Remains_Shutin

Friedrich, Mickey; Milliken, Mike (Aug. 2013) Determining the Contributing Reservoir Volume from Hydraulically Fractured Horizontal Wells in the Wolfcamp Formation in the Midland Basin. SPE 168839 / URTeC 1582170

Geological Society of America (Nov., 2012) GSA Geologic Time Scale. http://www.geosociety.org/science/timescale/timescl.pdf

Hoak, T., Sundberg, K., Ortoleva, P. (1997). Overview of the Structural Geology and Tectonics of the Central Basin Platform, Delaware Basin, and Midland Basin, West Texas and New Mexico. DOE/PC/91008—23-Pt. 8.

Schenk, C.J., Pollastro, R.M., Cook, T.A., Pawlewicz, M.J., Klett, T.R., Charpentier, R.R., and Cook, H.E., 2008, Assessment of undiscovered oil and gas resources of the Permian Basin Province of west Texas and southeast New Mexico, 2007, U.S. Geological Survey Fact Sheet 2007–3115, 4 p.

SEPM STRATA (2013, Feb. 13). *Permian Basin Chrono-Stratigraphic Cross-Section*. http://www.sepmstrata.org/page.aspx?pageid=138

SEPM STRATA (2013, Feb. 13). *A Brief Tectonic History of the Permian Basin*. http://www.sepmstrata.org/page.aspx?pageid=137

Shale Experts, Concho Resources (Jan., 2014) Shale Overview. http://www.shaleexperts.com/plays/wolfcamp-shale/Overview

Texas Railroad Commission (2014, Mar. 7). Permian Basin Information. http://www.rrc.state.tx.us/permianbasin/

Tim J. Hunt, Peter H. Lufholm (2003, Oct. 8-10). The Permian Basin: Back to Basics. West Texas Geological Society Publication #03-112.

Tom Deen, Valery Shchelokov, Ray Wydrinski, Tim Reed, Mickey Friedrich (Aug., 2013) Horizontal Well Performance Prediction Early in the Life of the Wolfcamp Oil Resources Play in the Midland Basin. SPE 168844 / URTeC 1582281

Troll, Ray (2009) Earth Time – National Science Foundation http://www.earth-time.org/trollart.html

Urbanczyk, Kevin, Rohr, David, White, John C. (1996) Geologic History of West Texas. https://www.twdb.state.tx.us/publications/reports/numbered_reports/doc/R356/Chapter2_3.pdf

US Department of Energy, National Energy Technology Laboratory (2013, Sep. 3). Permian Basin. http://en.wikipedia.org/wiki/File:Permian_Basin.jpg

Vertrees, Charles D. (2010, June 15). "PERMIAN BASIN," *Handbook of Texas Online* (http://www.tshaonline.org/handbook/online/articles/ryp02), accessed February 20, 2014. Uploaded on Published by the Texas State Historical Association.

Case Study References:

Passey, Q. R., Creaney, S., Kulla, J. B., Moretti, F. J., Stroud, J. D. 1990. A practical model for organic richness from porosity and resistivity logs. AAPG Bulletin, December, v. 74, p. 1777-1794.

Schmoker, J.W. 1979. Determination of Organic Content of Appalachian Devonian Shales from Formation Density Logs. *AAPG Bulletin*, **63**: 1504-1509.

Wang, F. P., and J. F. W. Gale, 2009, Screening criteria for shale-gas systems: Gulf Coast Association of Geological Societies Transactions, v. 59, p. 779-793.

Zhao, H., Givens, N. B., Curtis, B. April 2007. Thermal maturity of the Barnett Shale determined from well-log analysis. AAPG Bulletin, v. 91, p. 535-549, doi:10.1306/10270606060.